Roles of Double Low-Level Jets in the Generation of Coexisting Inland and Coastal Heavy Rainfall Over South China During the Presummer Rainy Season

R10229003 凌文海

Introduction

- The pre-summer heavy rainfall can be roughly classified in two 2 types according to the dominant dynamic forcing origin:

1) Subtropical synoptic weather systems (cold or quasi-stationary front, a low-level vortex and a shear line) (Ding, 1994: Huang, 1986)

— Distributed extensively over inland south China

2) Occurring in the warm sector, a couple of hundred kilometers away from the subtropical weather systems. (Luo et al., 2017)

— Located over coastal region, with a smaller horizontal but larger maximum.

Introduction

- Warm-sector coastal rainfall occurs either by its own or concurrently with synoptic rainfall over inland China (Li et al., 2020; Wu et al., 2020)

- Closely associated with 1) oceanic southerly airflows in the BL (Du & Chen, 2018…) 2) convectively generated cold pools (Liu et al., 2018…), 3) land-sea contrast (Chen et al.,, 2016), and 4) orographic lifting (Wang et al., 2014; Yu & Cheng, 2013).

- Inland rainfall is usually related to 1) tropical-originating low-level jets (LLJs) (Chen et al., 2017; Du & Chen, 2019b…), 2) local topographic lifting (Jiang et al., 2017), 3) surface heating, and 4) urban heat island effect interacting with sea breezes (Wu et al., 2019; Yin et al., 2020).

Introduction

- LLJs can be generally classified into 2 types according to their mechanisms:

- 1) Synoptic system-related LLJ (SLLJ)

➢ Wind speeds peaking in the 1~4 km height

➢ Closely associated with the development and movement of synoptic and mesoscale systems (Gao & Sun, 1984; Uccellini & Johnson, 1979)

➢ Transporting warm, moist air from the tropical, destabilizing the environment and providing convergence at the terminus of the SLLJs (Chen et al., 1994; Tao & Chen, 1987)

- 2) Boundary Layer jet (BLJ)

➢ Wind speed maximum in the BL

➢ By the inertial oscillation of ageostrophic winds (Blackadar, 1957) or baroclinicity associated with the terrain (Holton, 1967) or a combination of the two (Du & Rotunno, 2014; Du et al., 2014)

Introduction

- Southerly airflows in the BL from the northern South China Sea (SCS) are important to produce extremely heavy warm-sector rainfall over the south China coasts (Liu et. Al, 2018; Wang et al., 2014; Wu & Luo, 2016; Yin et al., 2020)

- Not necessarily reaching the BLJ's minimum intensity (peak wind speed > 10 m/s)

- Produce lifting that favors the generation of DC and helps maintain the rainstorms when the southerly flows in the BL encounters terrain, cold pool or the coastline. (Chen et al., 2014; Liu et al., 2018; Wu, Zhuang, et al., 2020)

- SLLJ (BLJ) are closely related to the inland synoptic (coastal warm-sector) heavy rainfall.

- The coupling of BLJs and SLLJs favors the initiation of coastal convection leading to warm-sector heavy rainfall over south China through BL convergence and low-to-mid level divergence. (Li et al., 2020; Zhang & Meng, 2019, Shen et al., 2020)

Data and Methodology

- Gauge-based rainfall observations by the South China Monsoon Rainfall Experiment (SCMREX)

- 17000 rain gauges with an average resolution ~10km

- Coastal box: 120 * 800 km^2 with 651 gauges

- Inland box: 400 * 800 km^2 with 3410 gauges
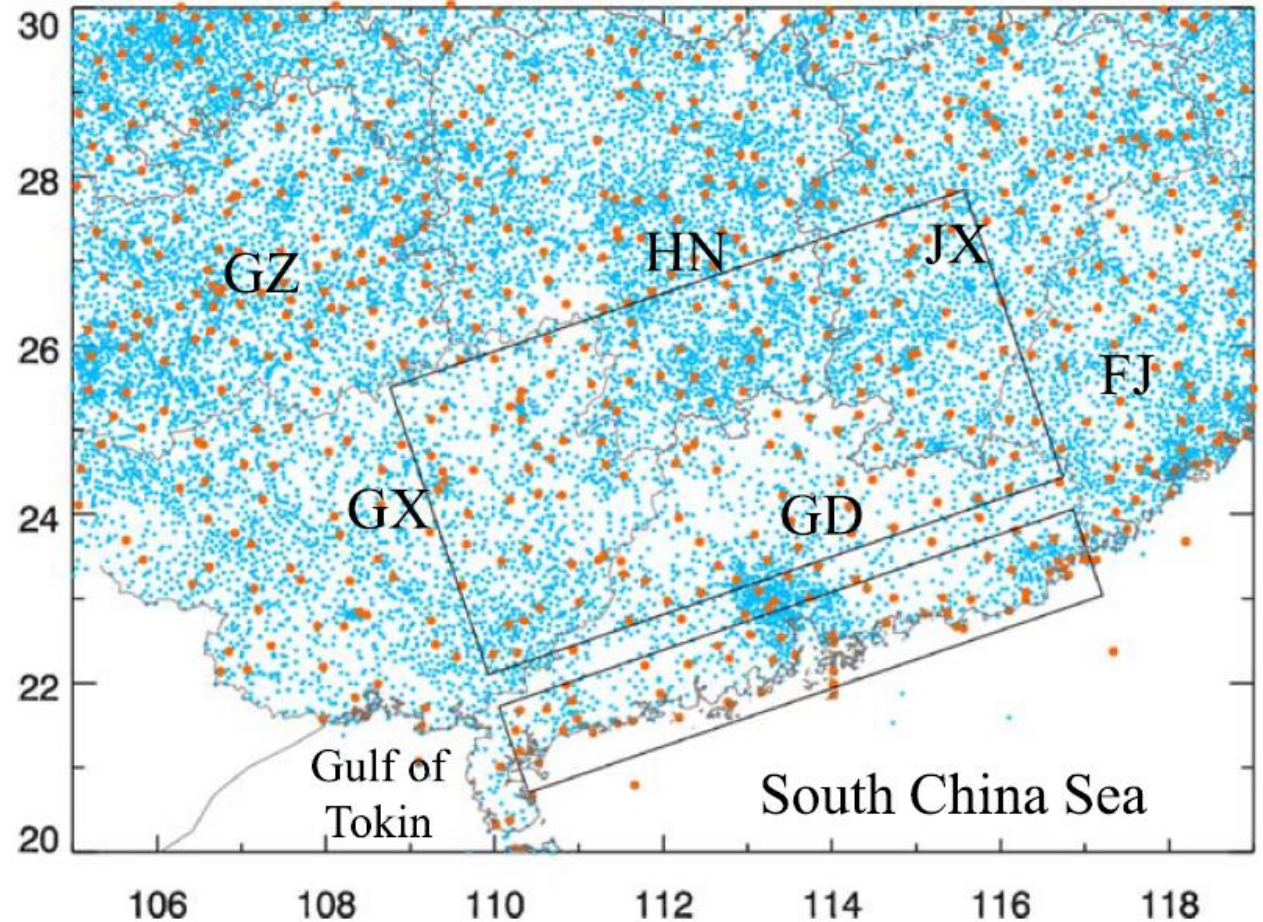
Data and Methodology

- PC: A day with more than 3 gauges in the coastal box observing the daily(local time) accumulated rain > 164mm [PR 99th of 87 national-level rain gauges in the coastal box during 1960-2014.]

- PI: A day with more than 300 gauges in the inland box observing the daily precipitation > 50mm [The heavy rainfall threshold used by CMA]

- A total of 10 events in Apr-Jun. 2011-2017 satisfied, 2 typhoon-induced cases excluded and 1 case with the coastal rainfall too close to the synoptic front/shear line.

Data and Methodology

- The ensemble forecasts with 0.5 horizontal resolution and 6hr intervals from ECMWF

- To reveal the relative importance of LLJs for coastal & inland rainfall via measuring linear relationships between rainfall and state variables through ensemble statistics.

- The Observing System Research and Predictability Experiment Interactive Grand Global Ensemble (TIGGE)

- 50 ensembles * 3 different initial times: 1200 UTC 2 days before, 0000 and 1200 UTC 1 day before the event dates.

Data and Methodology

- PC/PI : The area-averaged 6 hr accumulated precipitation from the ensemble forecasts over the coastal/inland regions.

- At certain grid point, the Pearson correlation coefficient is:

- $r = \dfrac{\sum_{i=1}^{n}(X_i - \bar{X})(P_i - \bar{P})}{\sqrt{\sum_{i=1}^{n}(X_i - \bar{X})^2 \sum_{i=1}^{n}(P_i - \bar{P})^2}}$

- P is the area-averaged 6 hr accumulated rainfall, X is the atmospheric variable of interest at certain forecast time at this grid point.

- The overbar represents the mean of the variable, n = ensemble size

- $|r| > 0.16$ is statistical different from 0 at the 95% confidence level using a two-tailed significance test

Data and Methodology

- The ECMWF reanalysis (ERA-Interim) with a 0.25° horizontal resolution and 6 hr intervals.

- Follow Whiteman et al. (1997):

- The synoptic low level jets (SLLJ) : peak wind speed > 10 m/s with vertical shear > 5 m/s in the 900-600 hPa layer.

- The boundary layer jets (BLJ) : peak wind speed > 10 m/s with vertical shear > 5 m/s beneath 900 hPa.

- In TIGGE (9 levels from 1000 to 100 hPa only)

- SLLJs (BLJs) are defined as the horizontal winds at 850 hPa (925hPa) with ensemble mean wind speeds > 10 m/s.

Data and Methodology

- Separate a mesoscale field (A')from the total field (A) using a simple mesoscale filter applied to the ensemble forecast data set.

- Tao & Xie (1989) showed that when this filter is performed 3 times to gridded data with a horizontal resolution < 100km, $\hat{A}$ could retain > 95% synoptic-scale information (~2000 km), and A' attains > 70% mesoscale information (~500 km).

- $A' = A - \hat{A}$, where $\hat{A}$ is the 9-point smoothing values with S = 0.5:

- $\hat{A}_{i,j} = A_{i,j} + \frac{S}{2}(1 - S) \times A1 + \frac{S^2}{4} \times A2$

- $A1 = A_{i-1,j} + A_{i,j-1} + A_{i+1,j} + A_{i,j+1} - 4 \times A_{i,j}$

- $A2 = A_{i-1,j+1} + A_{i-1,j-1} + A_{i+1+1,j} + A_{i+1,j+1} - 4 \times A_{i,j}$

Data and Methodology

- The obtained $\hat{A}$ field is used to calculate quasi-geostrophic ω by:

- $\left(\nabla^2 + \frac{f^2 \partial^2}{\sigma \partial p^2}\right)\omega = \frac{f}{\sigma}\frac{\partial}{\partial p}\left[V_g \cdot \nabla\left(\frac{1}{f}\nabla^2\varphi + f\right)\right] + \frac{1}{\sigma}\nabla^2[V_g \cdot \nabla\left(-\frac{\partial\varphi}{\partial p}\right)]$

- where f is the Coriolis parameter, φ is the geopotential height, V_g is the geostrophic wind, and σ is the static stability.

- An overrelaxation method is used to solve Poisson equation (Hu et al., 2017; Zhong et al., 2014)

- ω is set to 0 at the surface and 100 hPa in order to remove the effects of topographic and BL forcing on tropospheric vertical velocity.

Overview of the Coexisting Dual-Rainbelt Events

Table 1

A List of Six Rainfall Events and Their Relevant Information

#	Date of events (UTC)	Number of stations with daily rainfall meeting the thresholds in each box	The percentage of stations in each box that meet the thresholds (%) (coastal/inland)	Maximum daily precipitation (mm) over each box (coastal/inland)	Coexisting period of the two rainbands (UTC) (dd/hh)	Model-data analysis period (UTC) (dd/hh)
1	2013-04-30	4/399	0.61/11.7	309.5/256.5	30/00Z–30/08Z	30/00Z–30/06Z
2	2013-05-08	23/316	3.53/9.27	335.7/236.0	07/20Z–08/15Z	08/00Z–08/06Z
3	2014-05-11	63/808	9.68/23.7	431.4/184.3	10/19Z–11/06Z	11/00Z–11/06Z
4	2014-05-22	3/1223	0.47/35.87	506.5/321.9	21/12Z–22/00Z	21/18Z–22/00Z
5	2015-05-20	25/1124	3.84/32.96	553.1/386.4	19/12Z–20/01Z	19/18Z–20/00Z
6	2016-06-13	10/439	1.54/12.87	250.1/187.1	12/15Z–13/00Z	12/18Z–13/00Z

Note. Dates are formatted as yyyy-mm-dd.

- For each event, we focus on its first 6 hr development stage when both the inland & coastal rainbelts were present.

Overview of the Coexisting Dual-Rainbelt Events

- Inland heavy-rain producing storms are mostly SW-NE oriented.

- Case 2 has a shorter rainbelt and the least gauges (9.27%) of heavy rainfall.

- The coastal rainstorms develop locally and move slowly along the coastline

- Case 3 has 9.68% gauges recorded extreme rainfall in the coastal region.
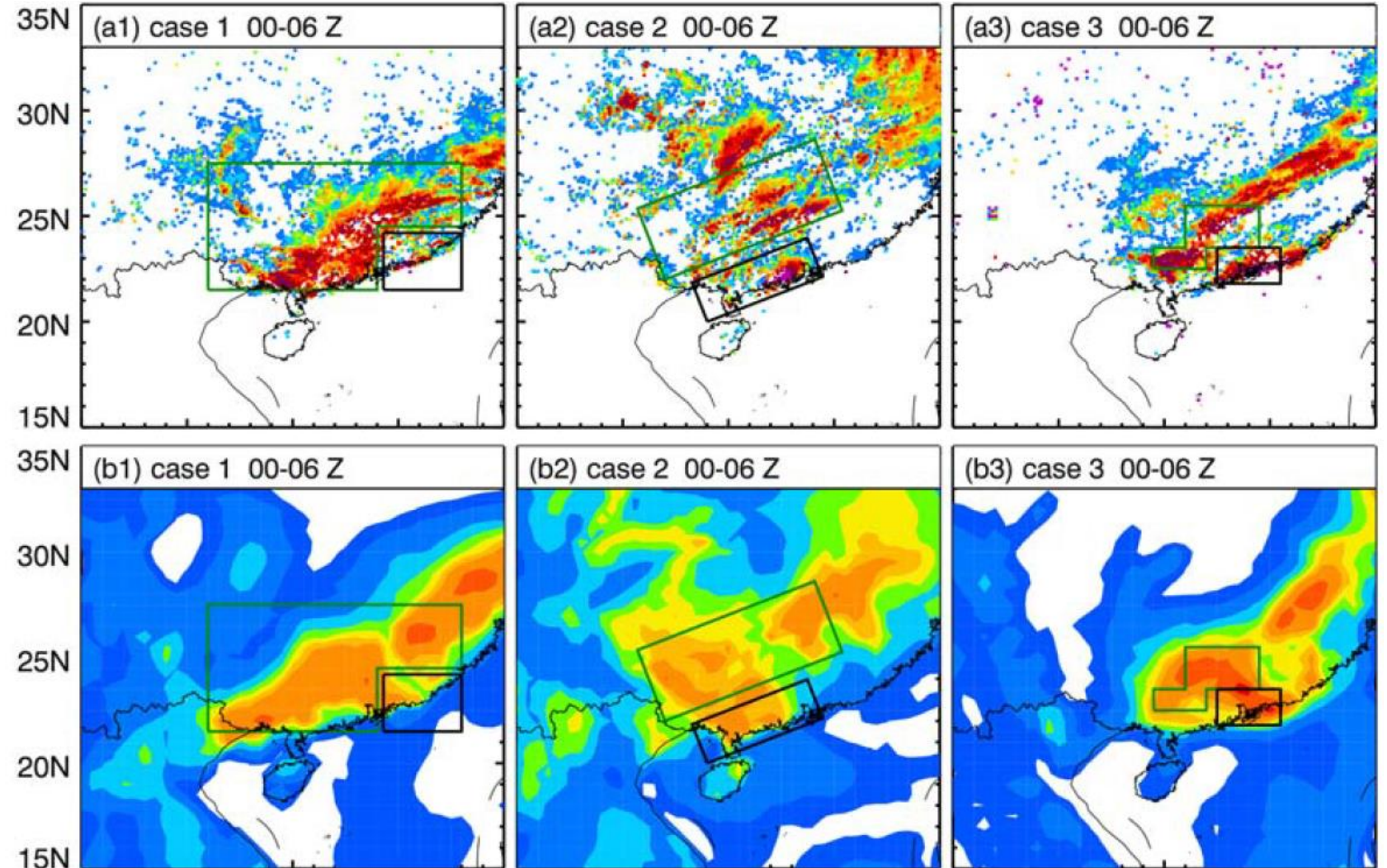
Overview of the Coexisting Dual-Rainbelt Events

Case 1

Case 2

Case 3

(a1) 00Z 30 April 2013
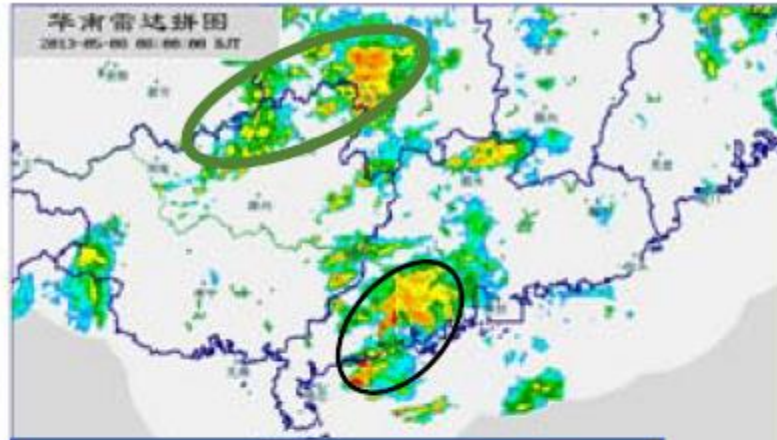
(a2) 00Z 8 May 2013
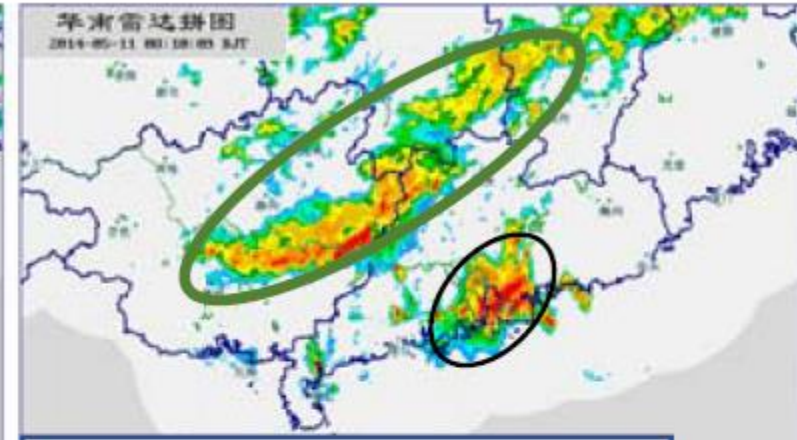
(a3) 00Z 11 May 2014

(b1) 06Z 30 April 2013

(b2) 06Z 8 May 2013
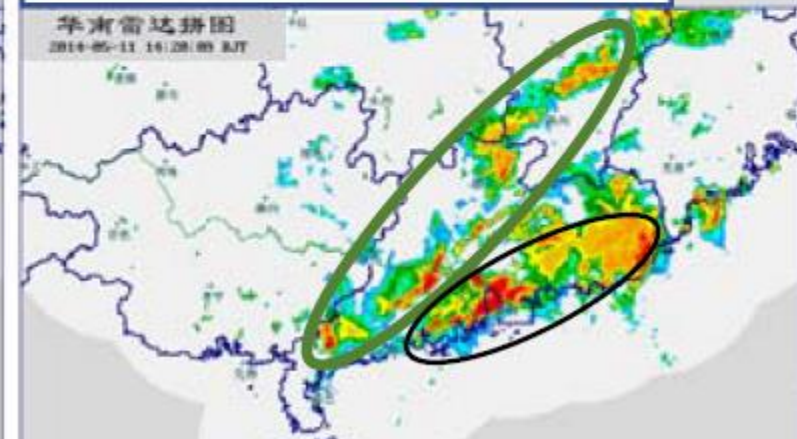
(b3) 06Z 11 May 2014

Overview of the Coexisting Dual-Rainbelt Events

- Case 4 has the widest inland rainbelt, with 35.87% of rain gauges recording heavy rainfall

- Inland Rainbelt Width:
- Case 4 > Case 5 > Case 3

- Only 3 gauges recorded in Case 4, but with 2nd 24 hr accumulated rainfall (506.5 mm) among 6 cases.
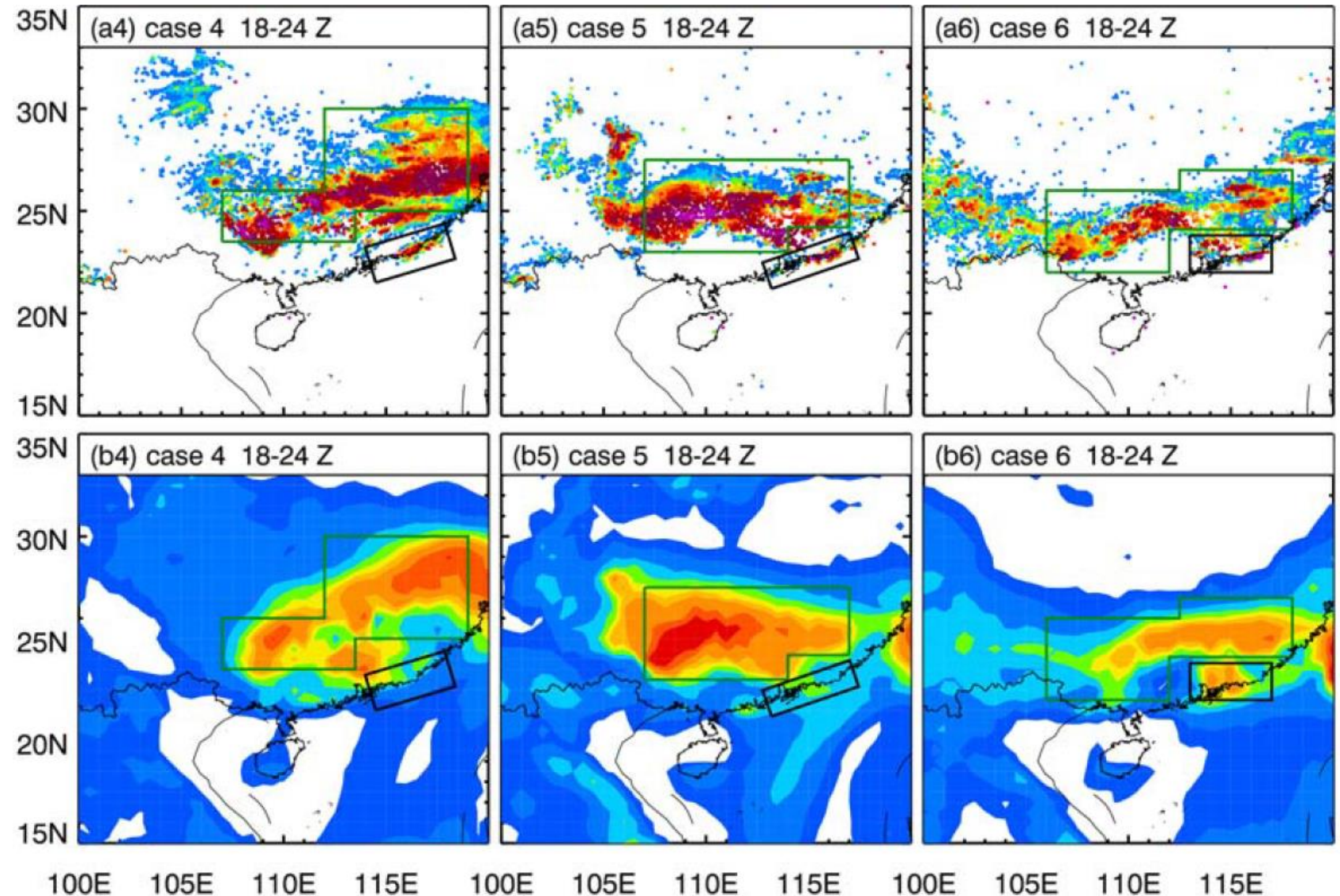
Overview of the Coexisting Dual-Rainbelt Events

Case 4

Case 5

Case 6
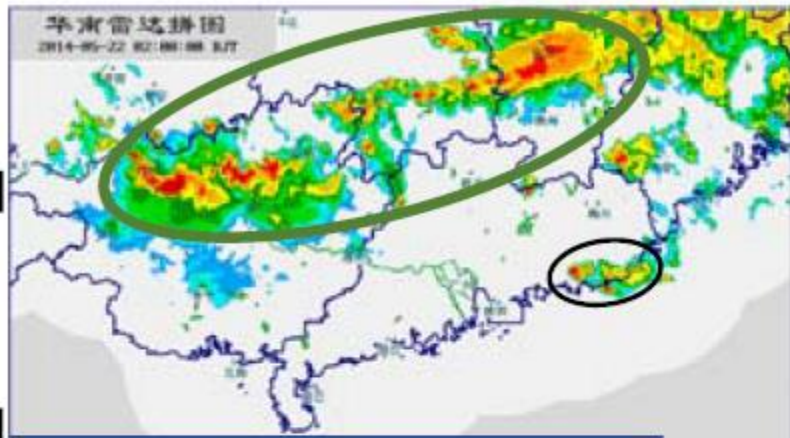
(a4) 18Z 21 May 2014
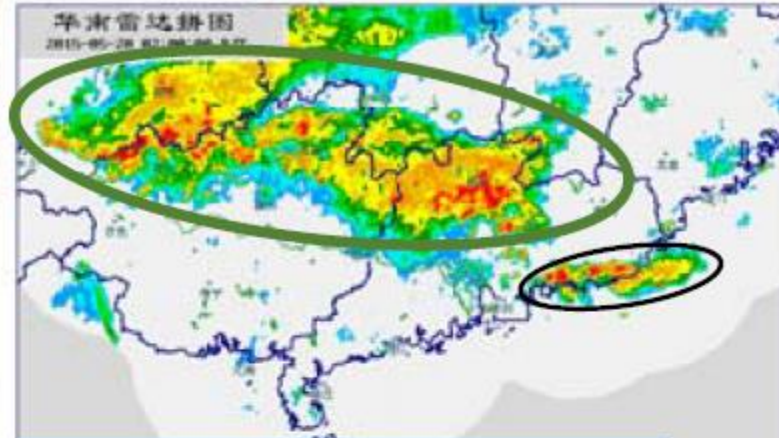
(a5) 18Z 19 May 2015
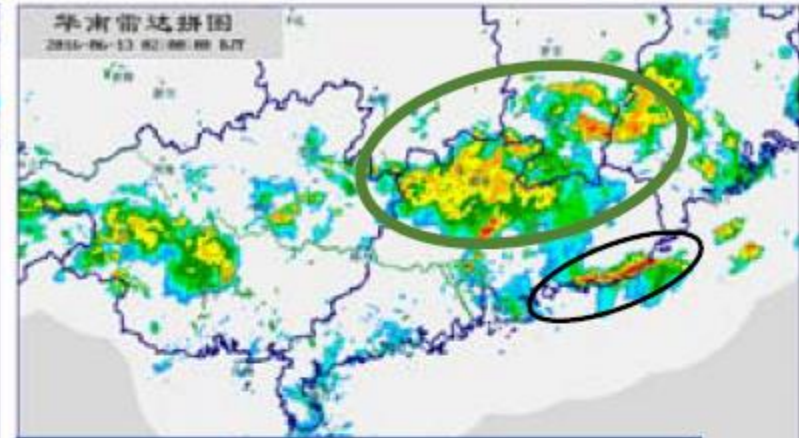
(a6) 18Z 12 June 2016
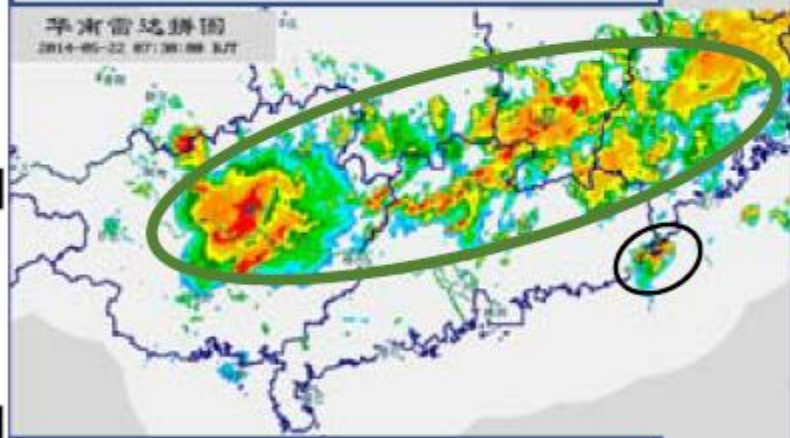
(b4) 00Z 22 May 2014
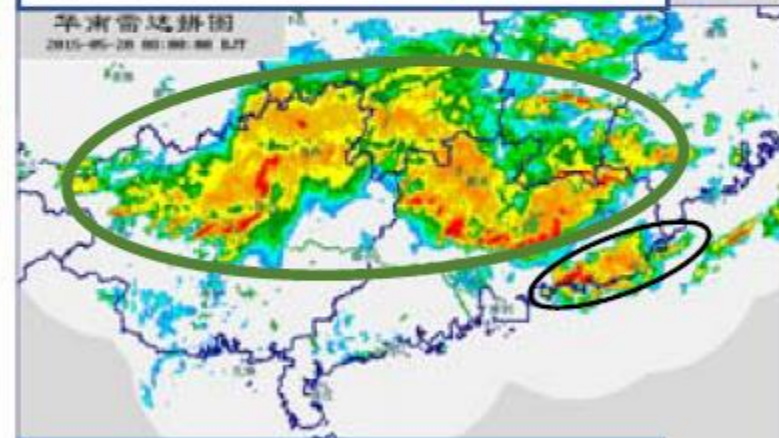
(b5) 00Z 20 May 2015
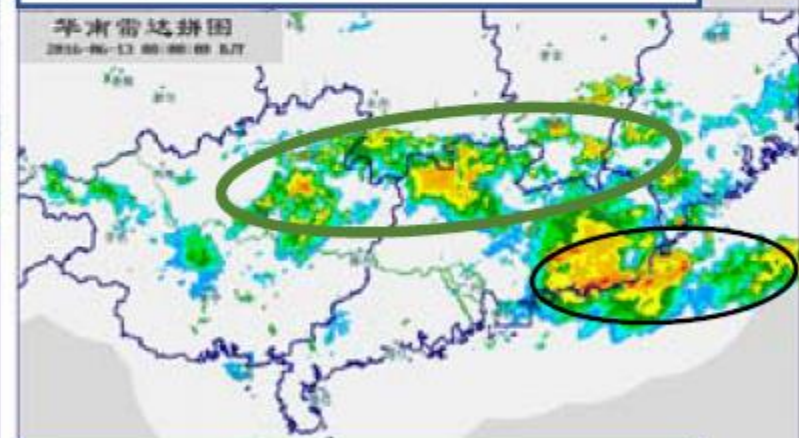
(b6) 00Z 13 June 2016

Overview of the Coexisting Dual-Rainbelt Events

The ERA-Interim analysis at the starting moments of model-data analysis period of the six events in Table

- The inland rainbelts are located close to a SW-NE oriented shear line at 850 hPa, with prevailing SW airflows of $\theta_e > 342$ K

- Case 1 & 2 before SCS monsoon onset : lower θ_e and weaker SW winds.
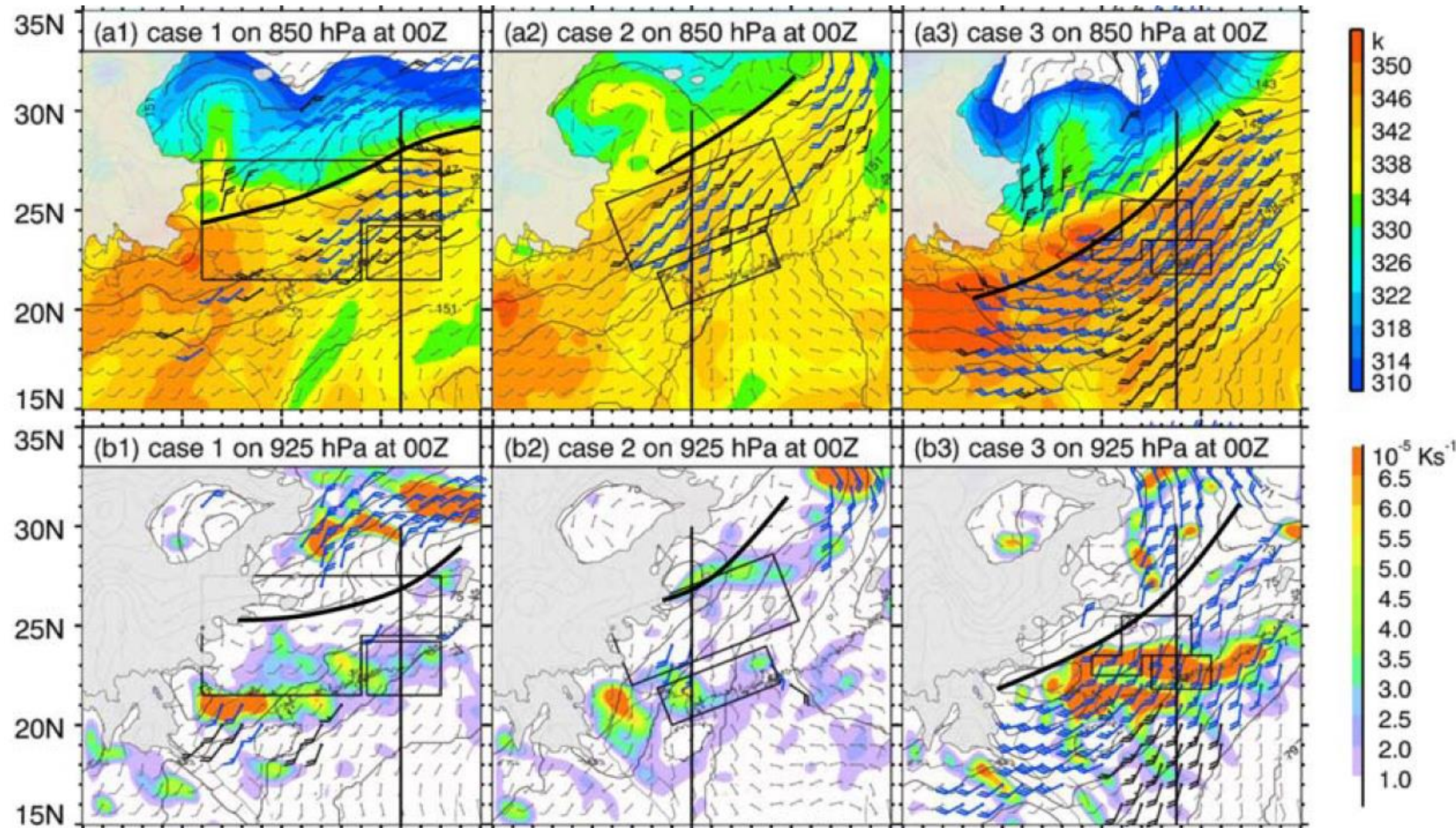
Overview of the Coexisting Dual-Rainbelt Events

- SW > 10 m/s observed @ 850 hPa ahead of cloud fronts or LL cyclone indicating the presence of an SLLJ related to the front and cyclone.

- Fronts @ 925 hPa are accompanied by strong SW winds over upstream regions.
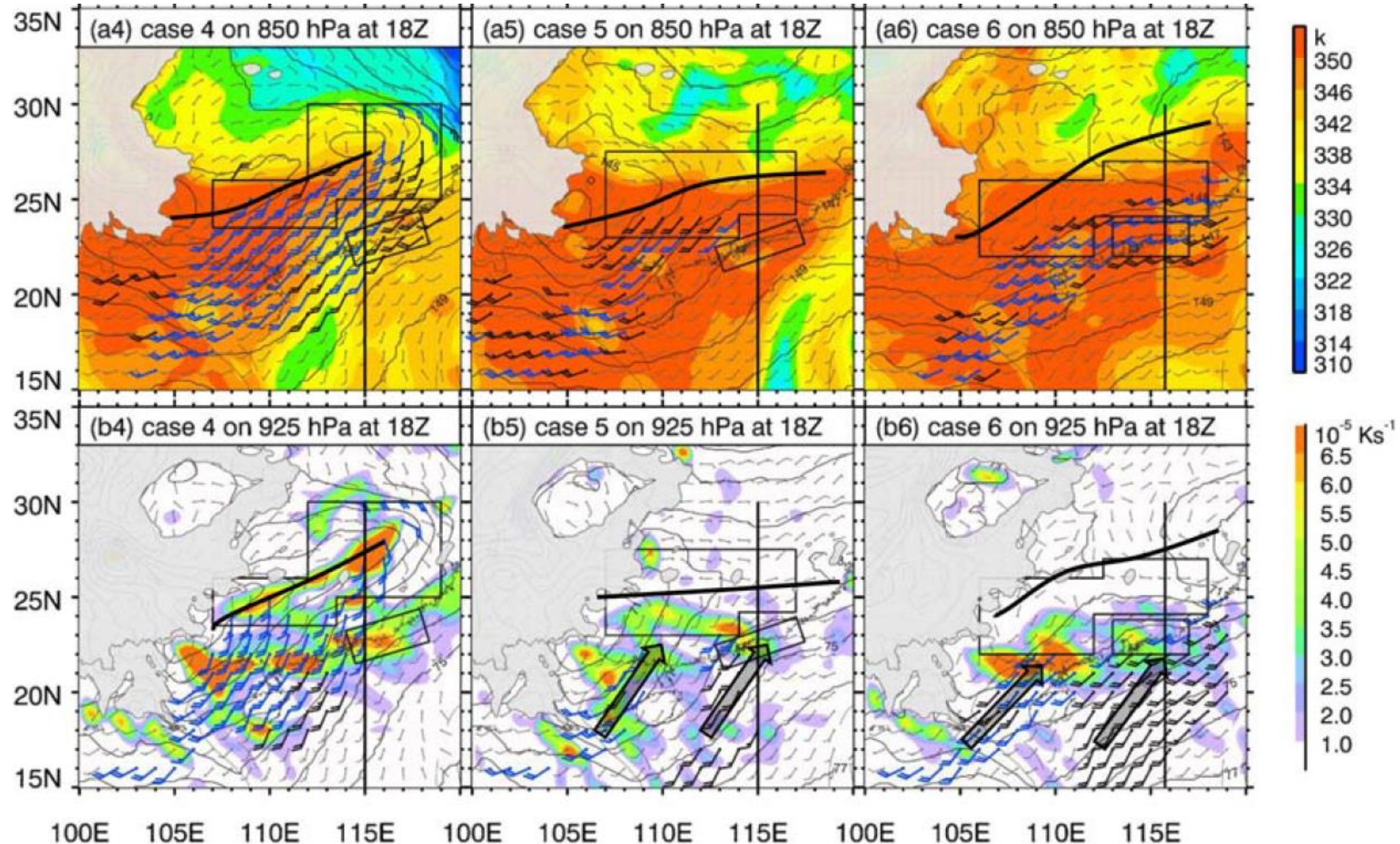
Figure 5. Vertical cross sections of meridional wind speed (shaded; m s^{-1}), meridional wind vector (arrows), and convergence and divergence of wind (black and white solid; contoured at intervals of 10^{-5} s^{-1}) along the

- The above analysis implies that the double LLJs (SLLJ and BLJ; Du & Chen, 2018) might occur over S. China in these 6 cases.

- Cross-sections of black line in last page.

- Case 2, 3, 4 : SLLJs occur to the S. of fronts/shear lines, with v > 12m/s in the 850-700 hPa layer.

- A large portion of the SLLJs in Case 5, 6 is composed of u.

- Case 3, 4, 5, 6 : BLJs over N. SCS with wind max. in 1000-900 hPa.

- Case 1, 2 : relatively weaker BLJs (before the Monsoon Onset)
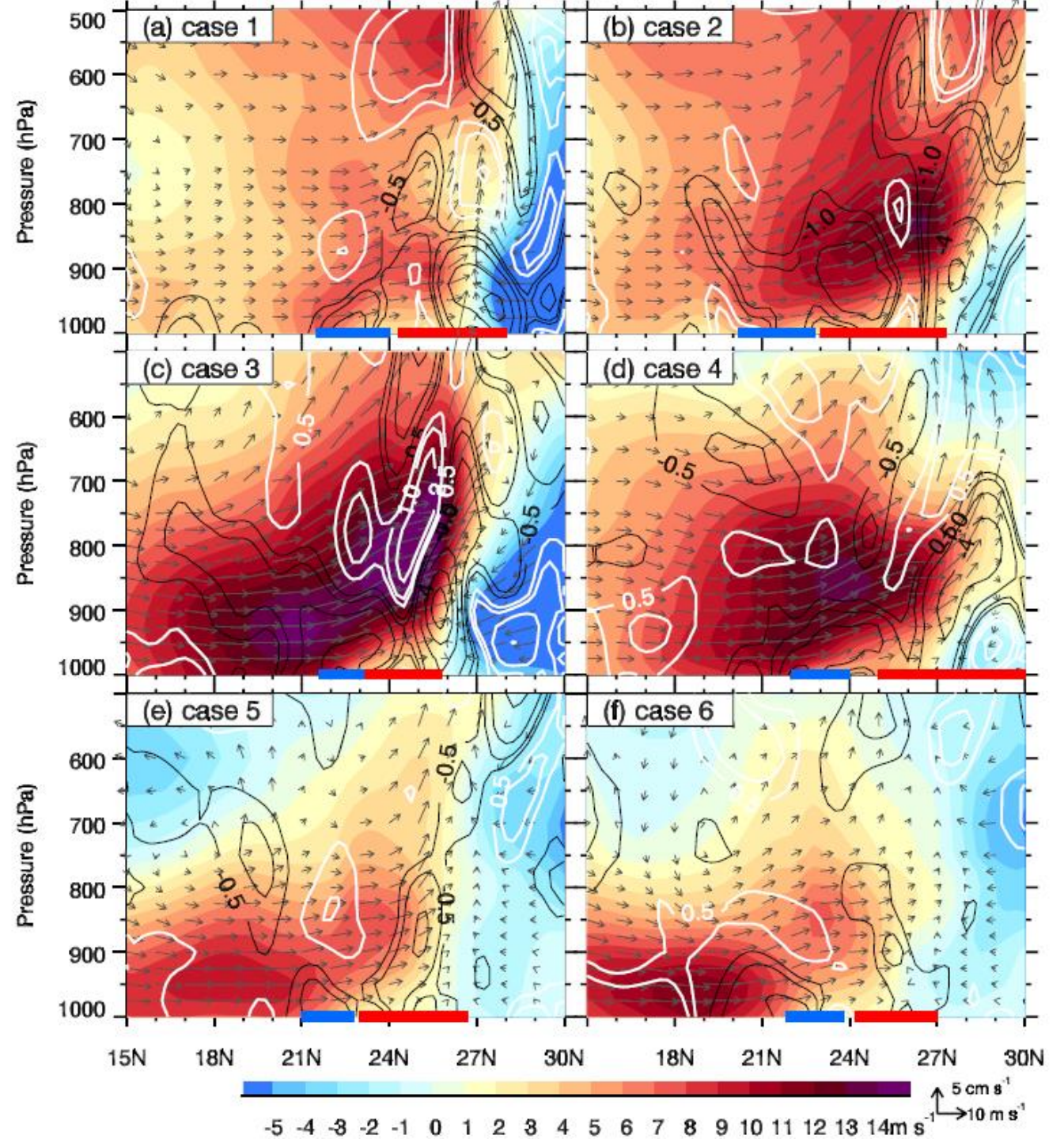
Ensemble Sensitivity Analysis of Winds - PI

- Liner correlations of PI & the v in the ensemble members

- High positive correlations between PI & v @ 850 & 925 hPa over the S. inland regions and N. SCS in all 6 cases

- Lower negative correlations are in N/NW inland

- Sharp deceleration of LL S. winds or strong convergence over inland regions are favorable for the PI.
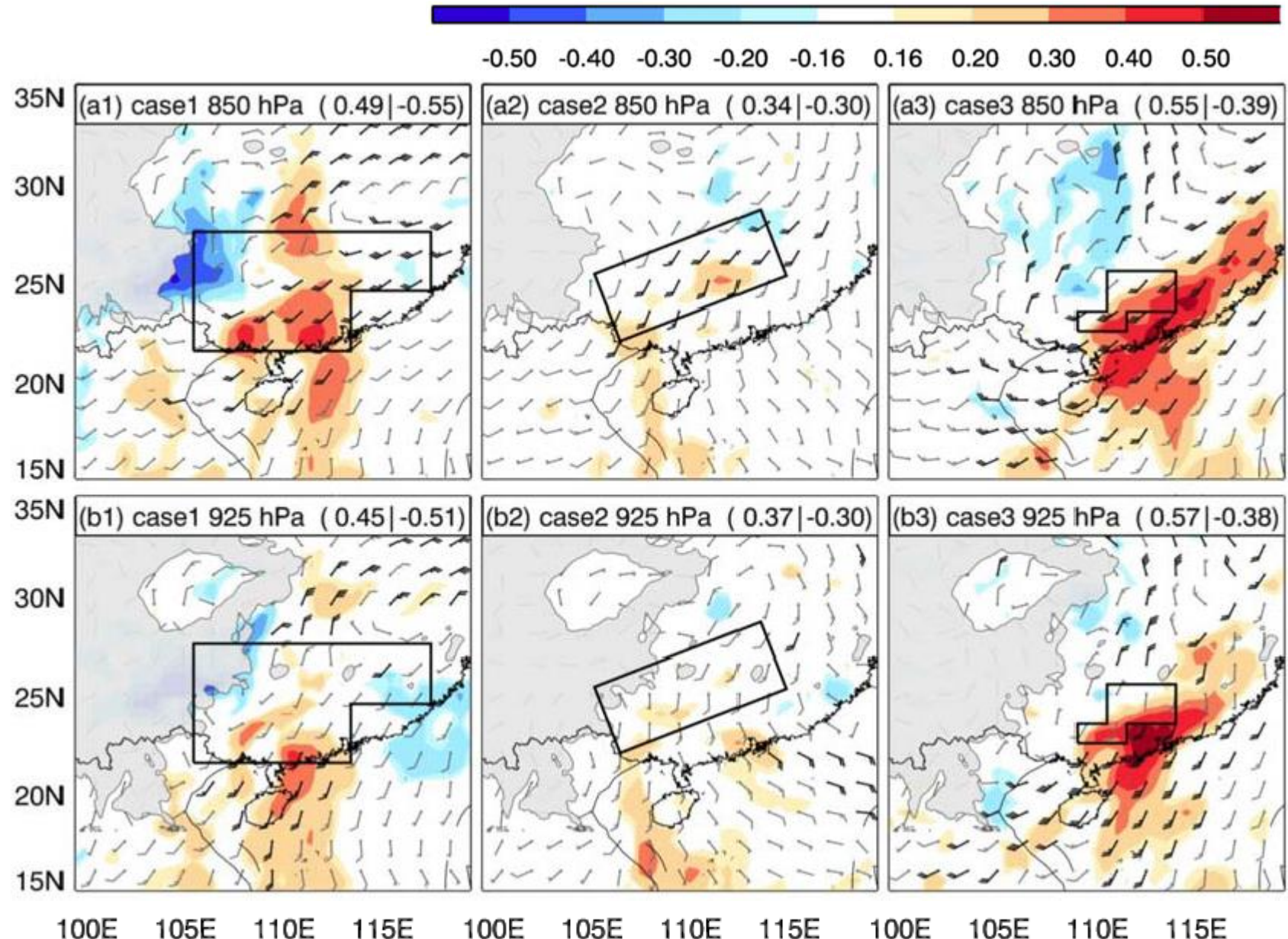
Ensemble Sensitivity Analysis of Winds - PI
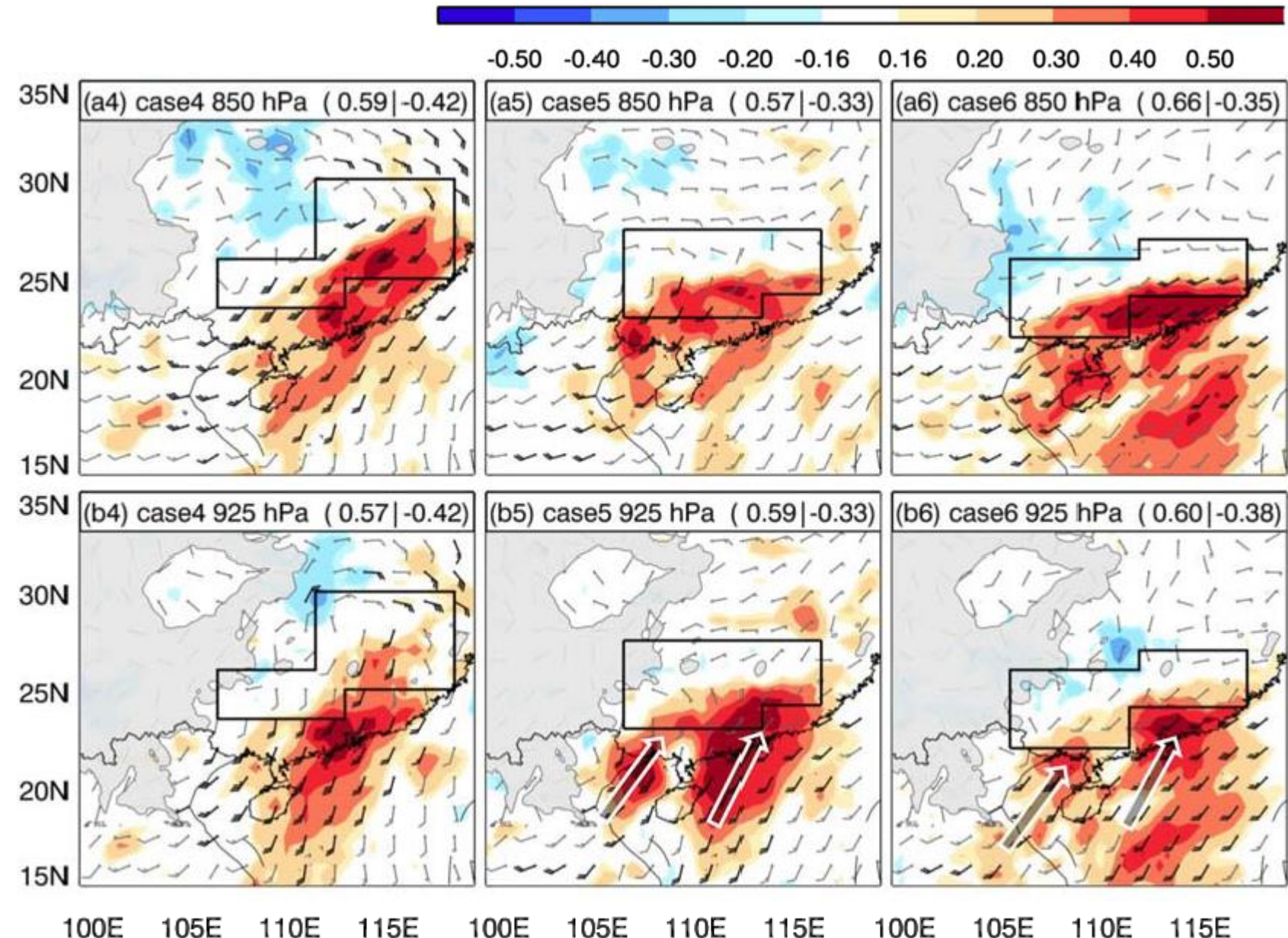
Ensemble Sensitivity Analysis of Winds - PI

- Liner correlations of PI & the u in the ensemble members

- u @ 850 – 925 hPa SW of inland regions are positively correlated, while negative correlations are distributed mostly over the sea SE of the inland region.

- Stronger (weaker) westerly flows on the west (SE) of the inland regions at the low levels contribute to heavier PI by strengthening convergence therein.
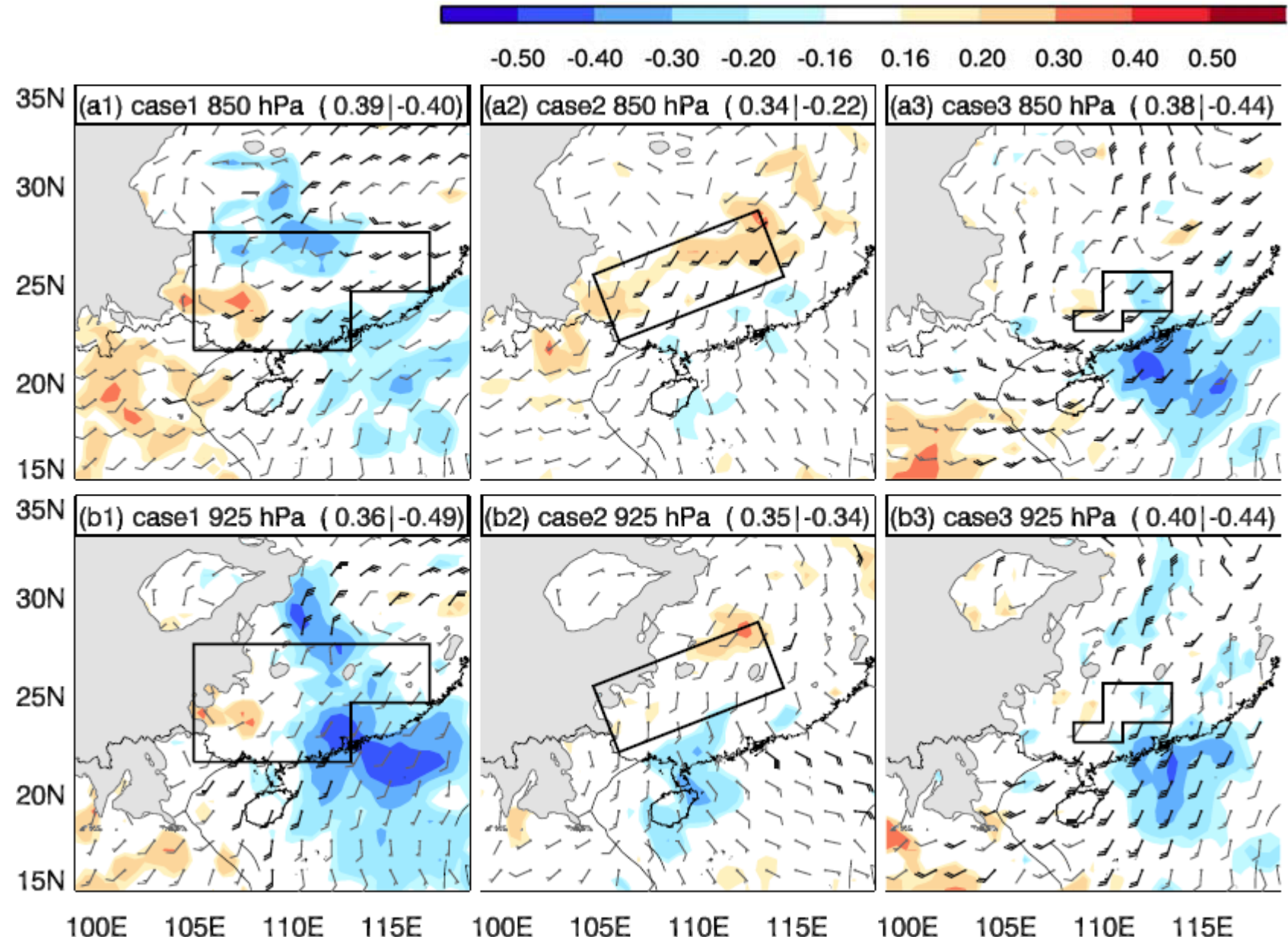
Ensemble Sensitivity Analysis of Winds - PI

- v is more important than u.
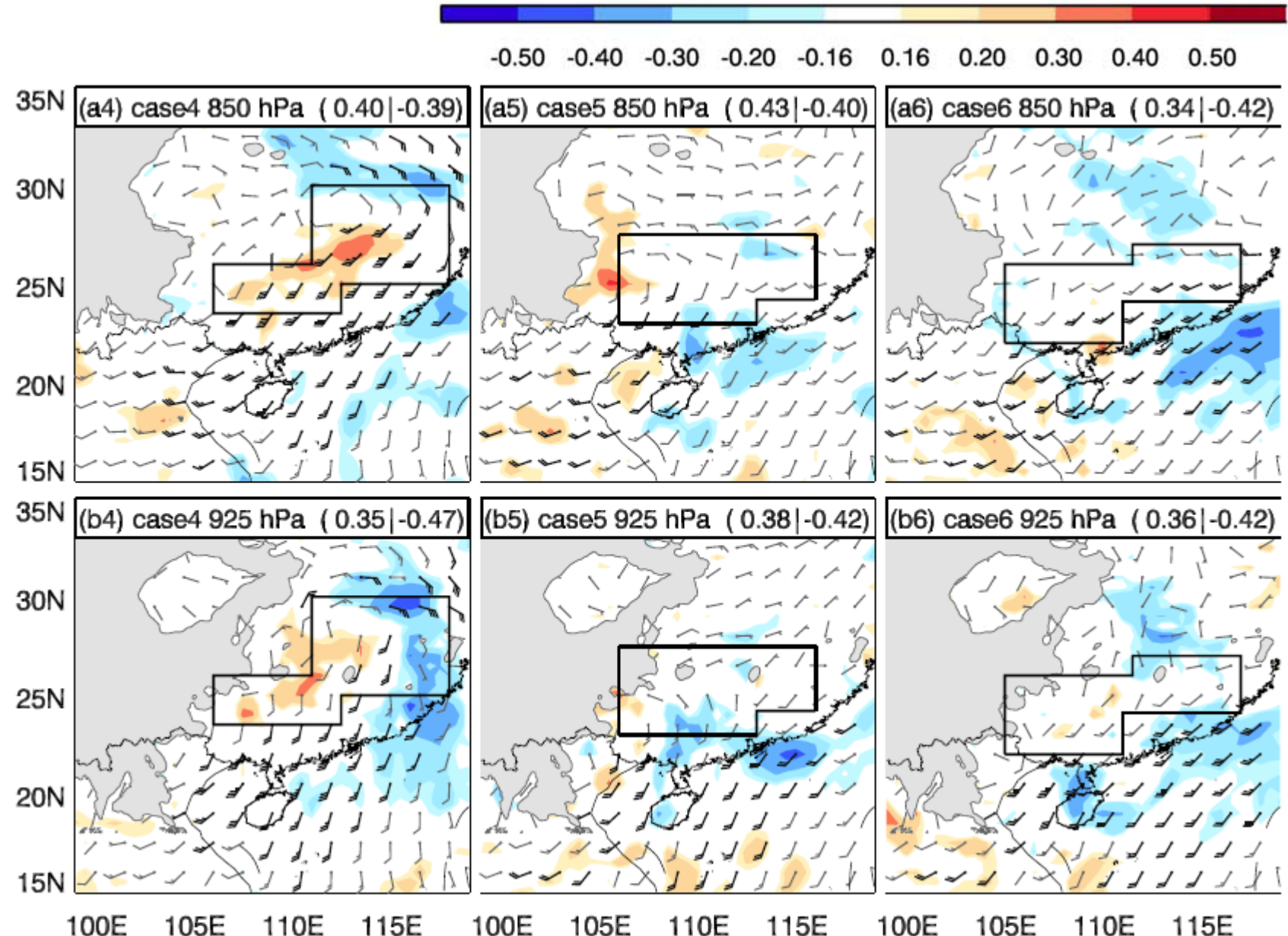
Ensemble Sensitivity Analysis of Winds - PC

- Linear correlations of PC & the v in the ensemble members

- Positive correlations between PC & v @ 850 and 925 hPa are found S. of the coastal region and N. SCS.

- Positive corr. Are higher and cover larger areas @ 925 hPa.

- Southerly flows in the BL over the N. SCS are more closely associated with heavier PC.
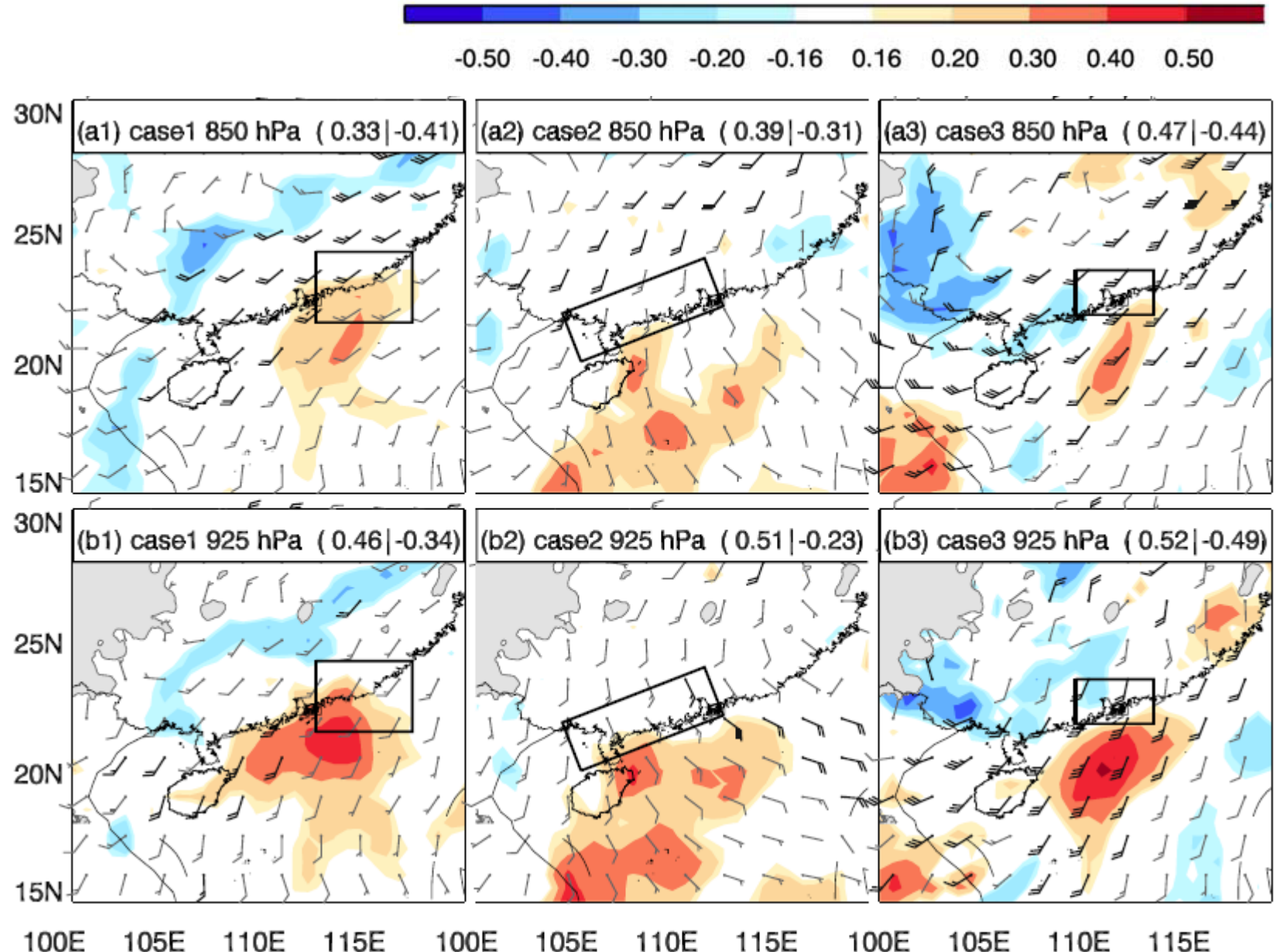
Ensemble Sensitivity Analysis of Winds - PC

- Areas of negative correlation are located N/NW of the coastal regions in Case 1, 3, 4, 5

- PCs are partly associated with enhanced convergence of stronger N. winds.

Ensemble Sensitivity Analysis of Winds - PC

- Liner correlations of PC & the u in the ensemble members

- Postive (Negative) Corr. With PC in SW (E) of the coastal regions.

- Indicate significant positive correlations between PC and the BL wind convergence.
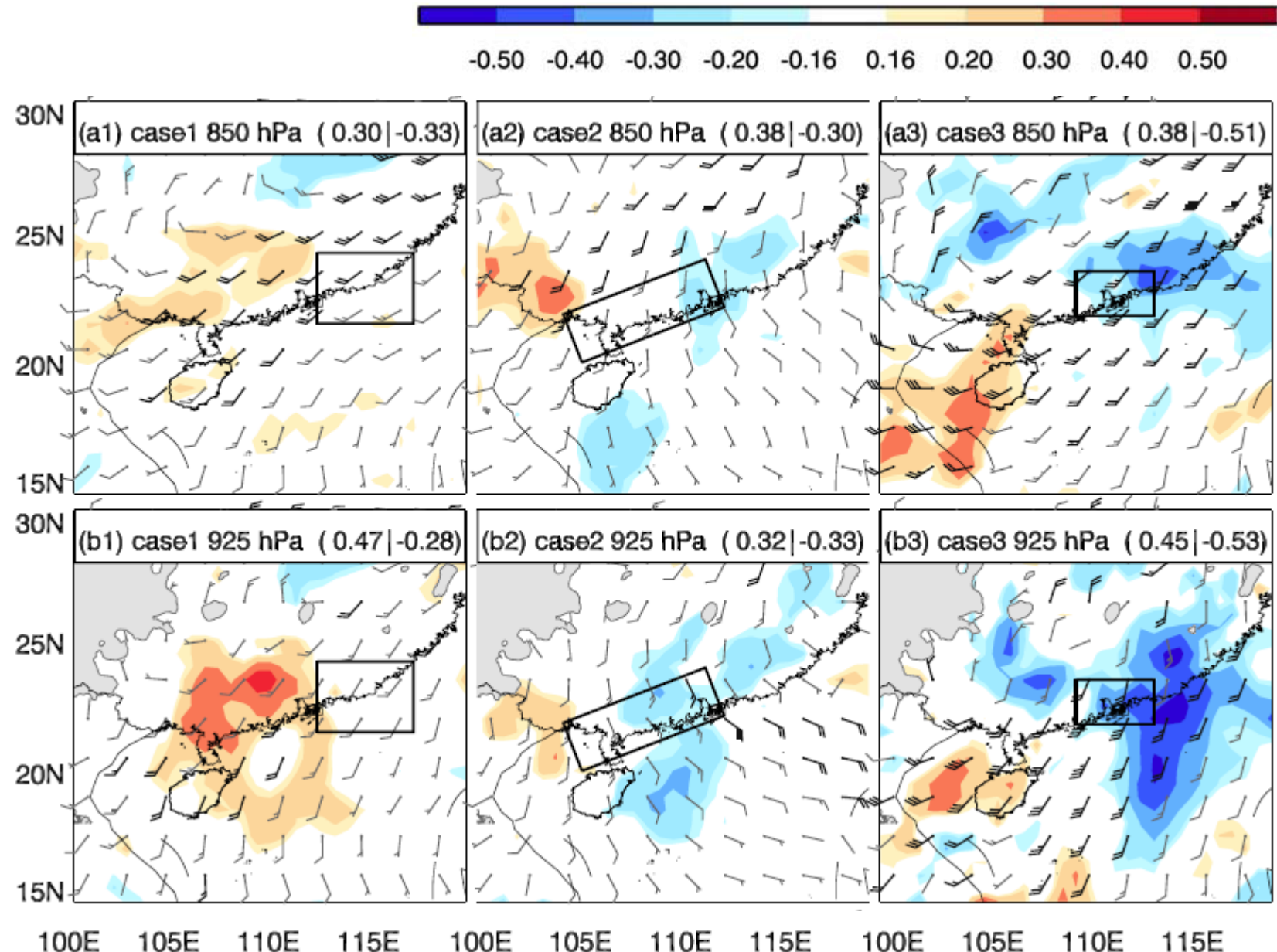
Ensemble Sensitivity Analysis of Winds - PC
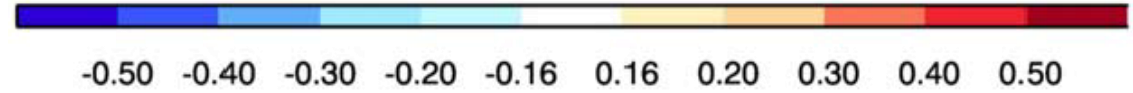
- Consistent with previous studies, showing that the BL S. flows play a key role in the initiation and development of rainstorms at the S. China coasts.

- Stronger winds are distributed more N. over the land @850 hPa than 925 hPa, due likely to the lack of frictional effects above the BL.
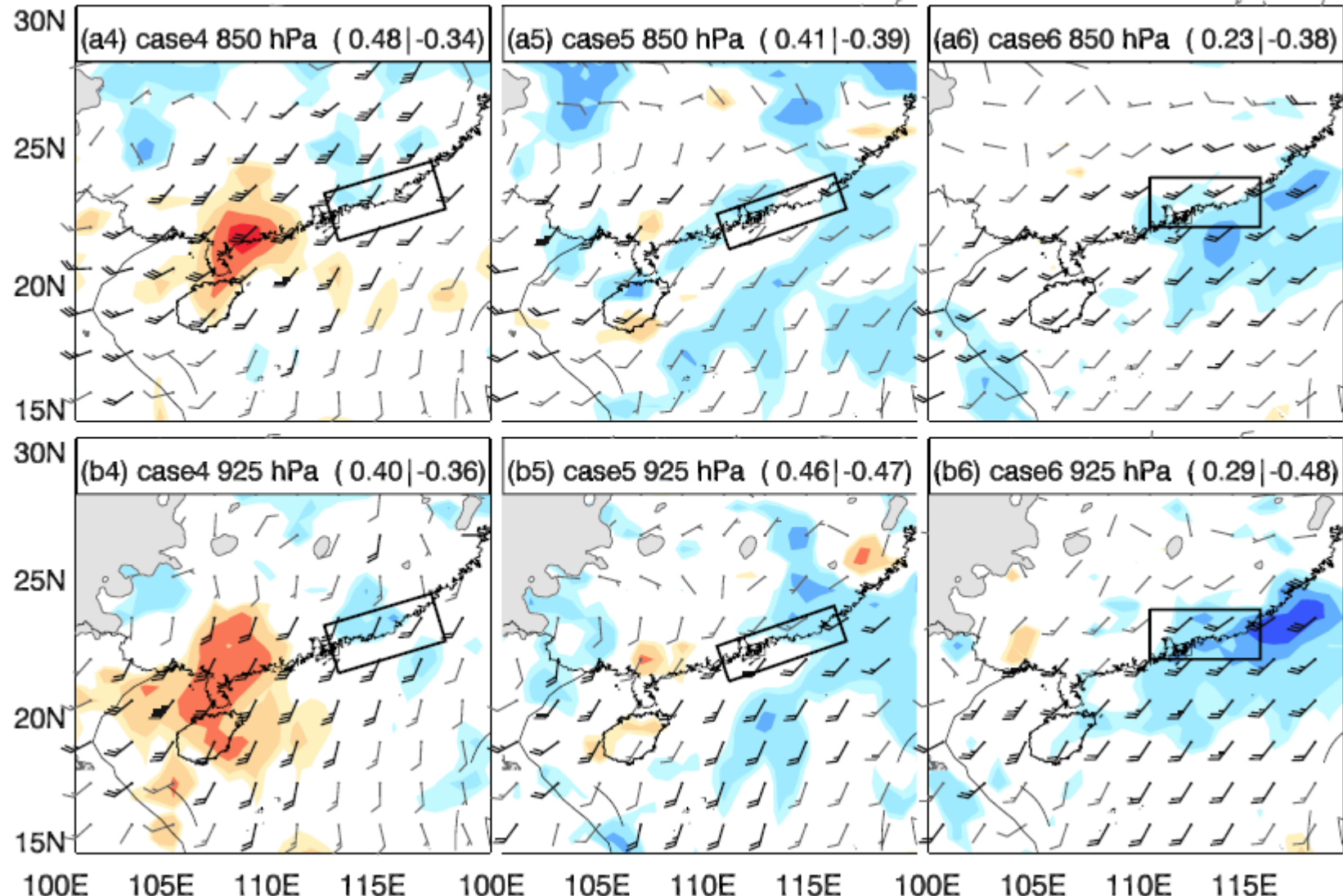
- The BL convergences appears at the N. terminus of the BLJ near the coast, with weak divergence above (850 – 700 hPa layer) at the entrance of the SLLJ.

- This coupling of BL convergence and divergence aloft near the coast is associated with the SLLJ-BLJ juxtaposition, corroborates the previous finding of Du and Chen (2019a)

- PC is more closely related to the BL flows, and also associated with the SW flows in the lower troposphere but with a lower correlation.
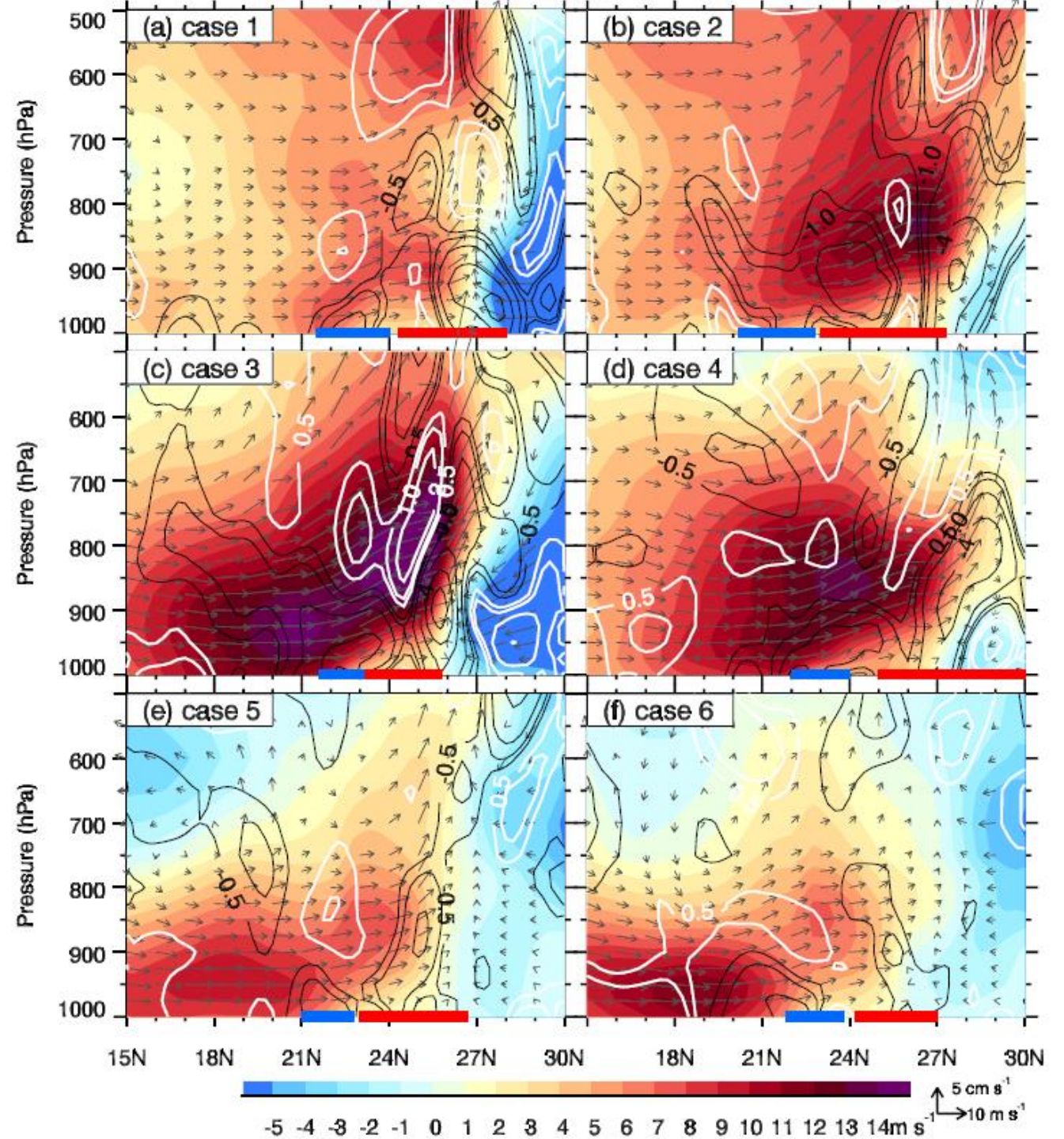
Dynamic Origins of Double LLJs Influencing Rainfall Production

- 30 members with the highest (lowest) values of predicted PI (PC) are identified as the good (bad) members for the inland (coastal) rainfall forecasts.

- The inland rainbelts in the good members of PI forecasts are quite close to the observations.

- The bad members of PC & PI with smaller magnitude than observations are due to the coarse resolution. (Gopalakrishnan et al., 2011; Kumar et al., 2015)

- Intensities and locations of the coastal rainbelts in the good members of PC are different from the observations.

- Lower predictability associated with the coastal rainfall than the inland rainfall.

Dynamic Origins of Double LLJs Influencing Rainfall Production

- Considering the high correlations of meridional winds (V) with both PI and PC, differences in V at 850 & 925 hPa between the composites of good and bad members (good – bad) are examed.

- As PC is more sensitive to V at 925 hPa than 850 hPa, the V difference maps at 925 hPa are shown.

- Only positive V differences are presented in this section since the positive correlations of V with PI and PC are much more evident.

PI

- The positive differences of full V associated well with the SE SLLJs and BLJs.

- Positive differences ~ 2.5 m/s and max. > 4 m/s, results in larger BL convergence over the inland region in the good members than in the bad members.

- The positive differences of full V are mainly contributed by those of geostrophic V in all cases.

- The ageostrophic V differences contribute less.
- In Case 1~4, the positive differences of ageostrophic V are limited in small areas
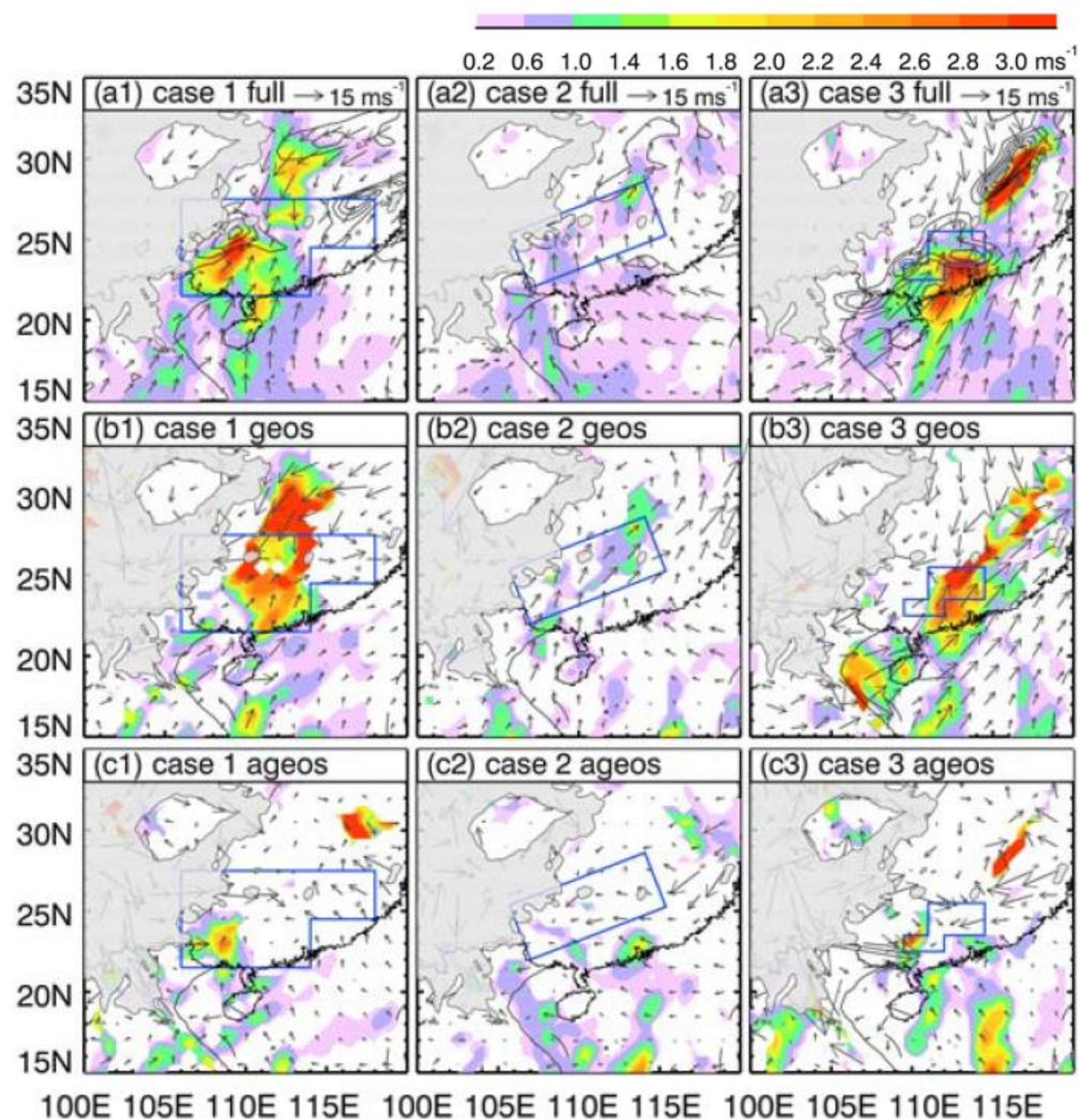
PI

- Differences between good and bad members are smaller in Case 2: consistent with the relatively weaker low-level cyclonic circulations and associated S. or SW winds, and lower correlations between meridional/zonal winds and PI.

- But the positive differences of geostrophic V are still mainly contributed by the positive differences of geostrophic V.

- The significant influences of strong southerly geostrophic wind on the inland synoptic heavy rainfall, even when the SLLJs and BLJs are not strong.
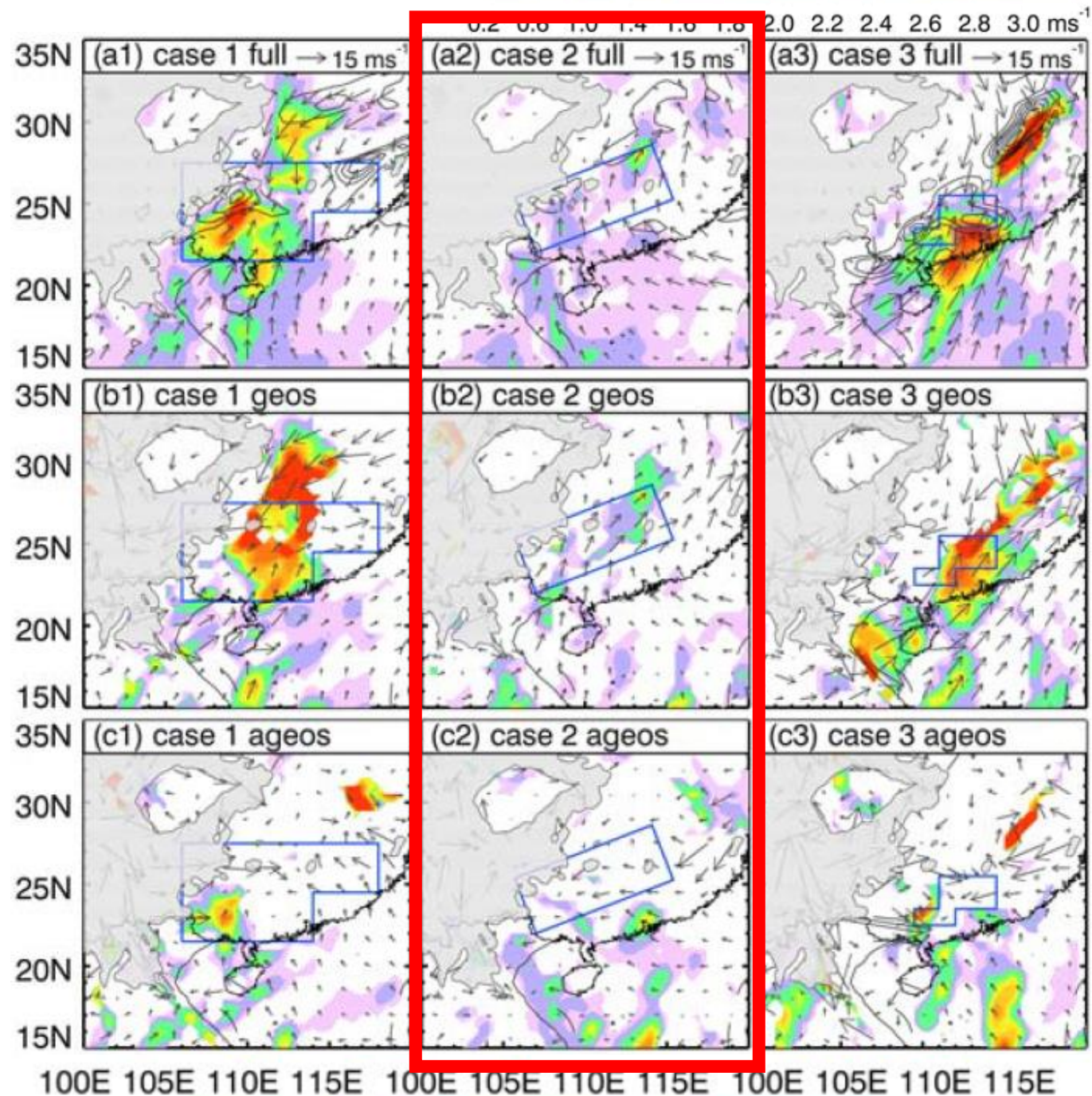
PI

- In Case 5,6 the ageostrophic V differences make evident contributions (~ 3m/s) to the full V differences over the areas SW of the inland regions.

- Corresponding to the left channel of the BLJ and associated SLLJ that are less correlated with PI compared with the right channel.

- Indicates the nonnegligible, albeit limited, influences of ageostrophic meridional winds on the forecasts of PI.
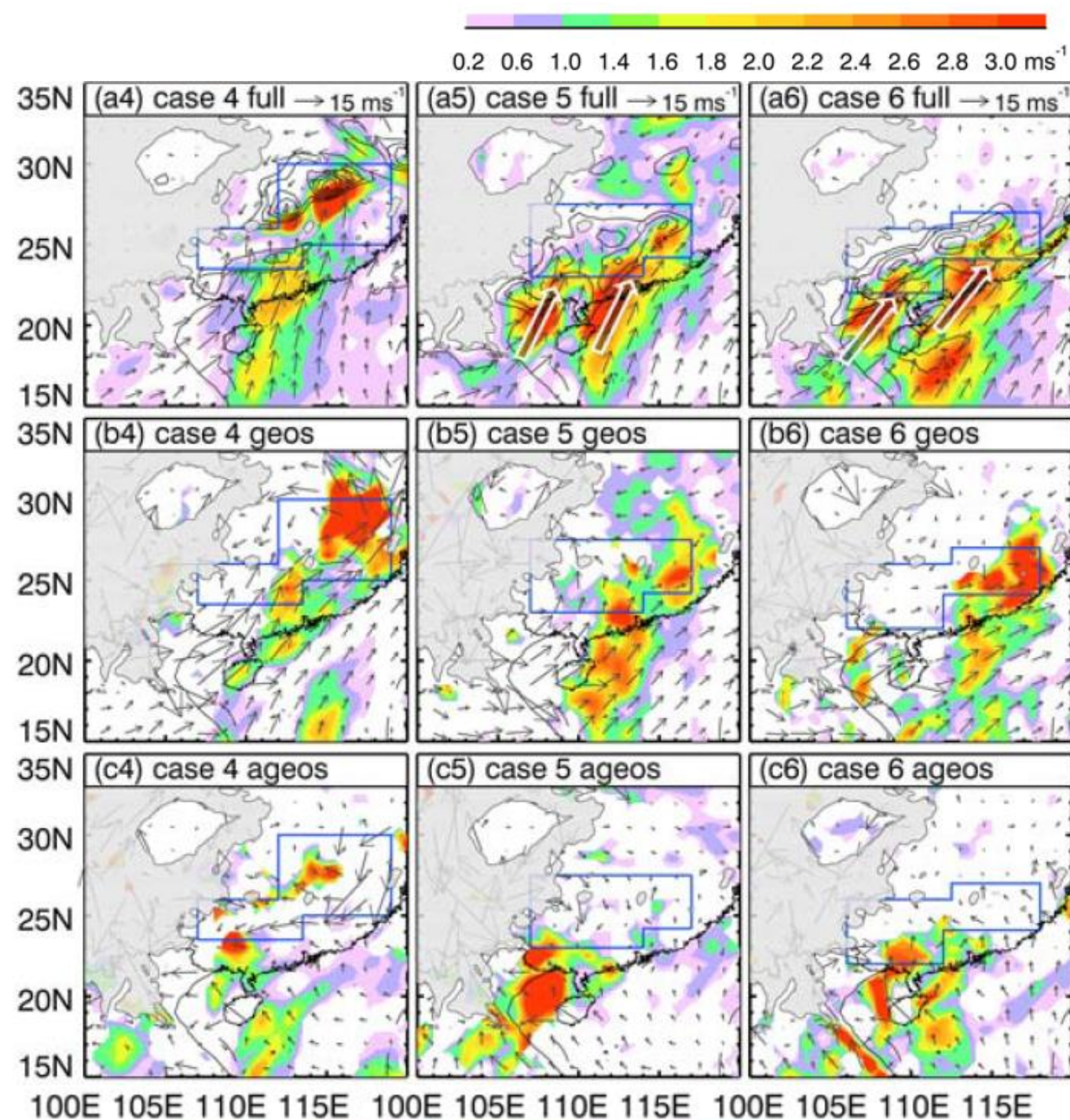
Dynamic Origins of Double LLJs Influencing Rainfall Production

- The quasi-geostrophic upward motions at 850 hPa are mostly distributed over the inland regions, ahead of the LL front/shear lines.

- PI is more directly related to the geostrophic wind component closely associated with the synoptic weather systems.

Quasi-geostrophic vertical velocity (shadings; Pa s−1) and equivalent potential temperature (solid contours at intervals of 4 K) at 850 hPa on the starting moments of the model-data analysis periods of the (a–f) six cases, averaged from 30 good members of each case. Gray shadings denote the areas with terrain height above 850 hPa.
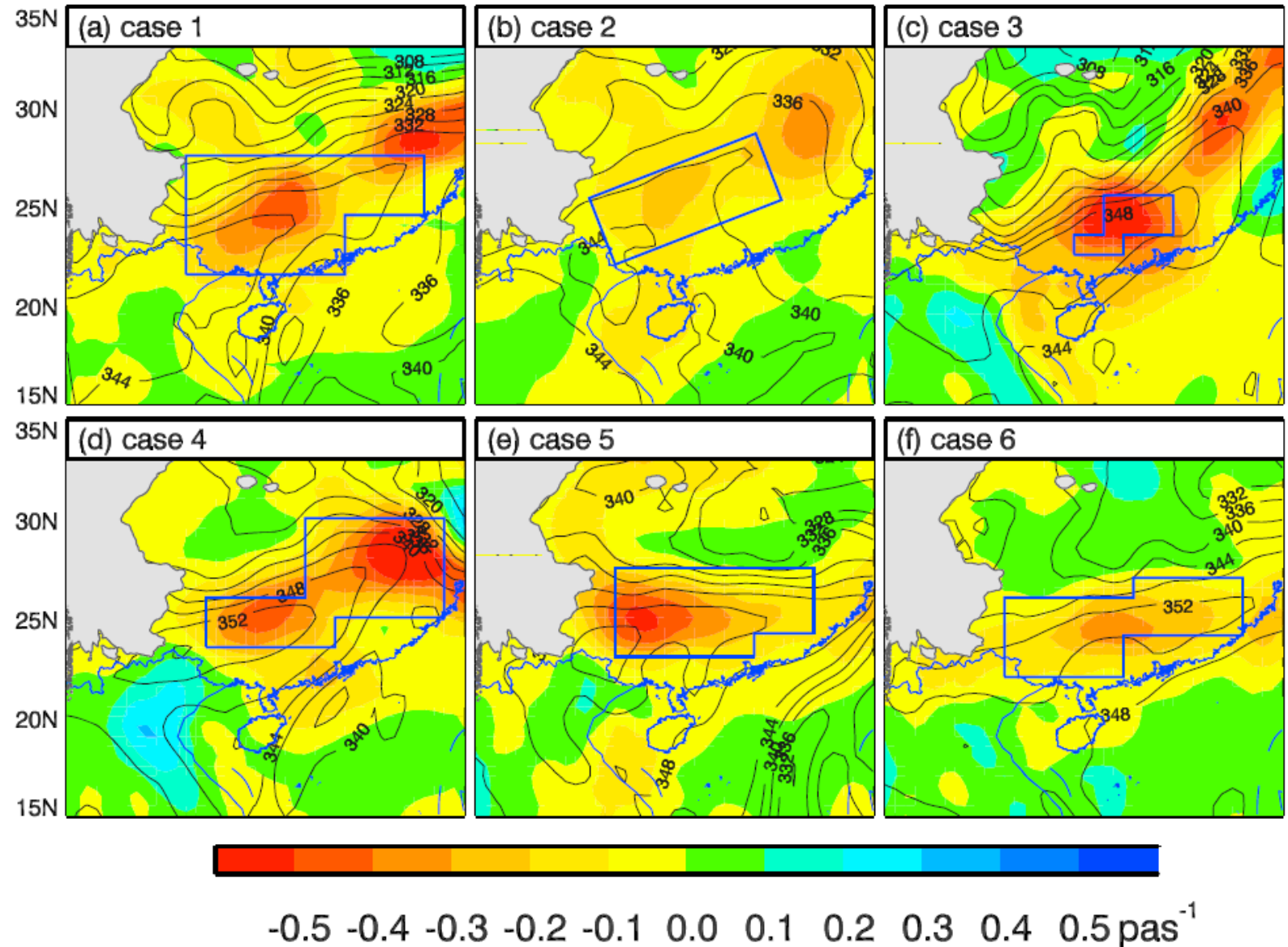
PC

- The positive differences of full V between good and bad members over the N. SCS, which is consistent with the distributions of PC and meridional wind correlations corresponding to the BLJ at 925 hPa.

- The positive differences of full V (0.6 ~ 2.8 m/s) would increase the convergence at the exit zone of the BLJ in the good members by about 0.2 ~ 1E-5 1/s.

- Stronger convergence over the N. terminus of the BLJ enhances the rainfall production over the coastal regions (Zhang & Meng, 2019)
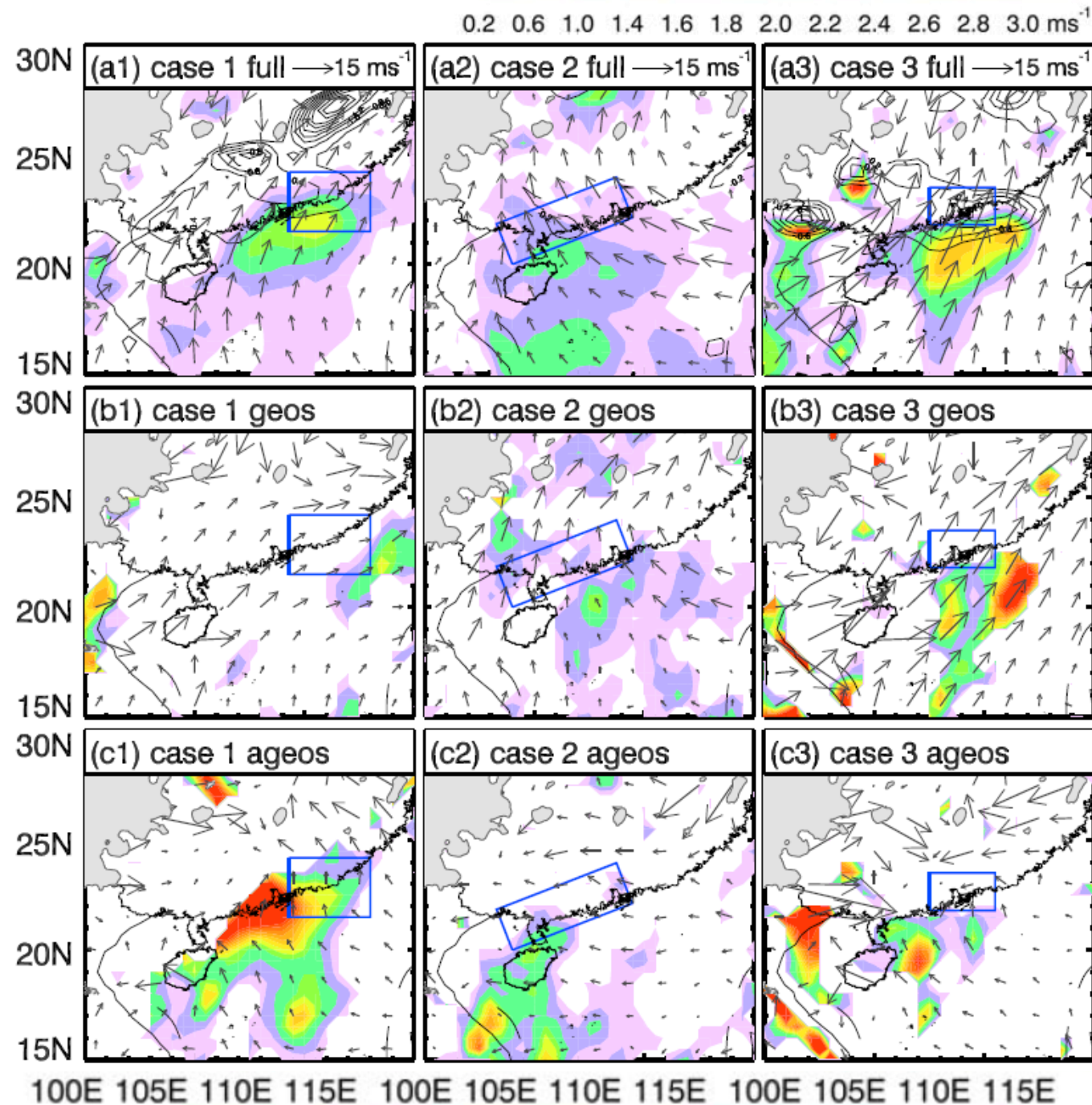
PC

- Neither the geostrophic nor ageostrophic V difference makes an overwhelming contribution to the positive full V difference upstream of the coastal region.

- Consistent with the generally weak quasi-geostrophic ascending motion over the coastal region.

- The ageostrophic winds contribute a lot to the meridional wind speed in the BL that is highly correlated with PC.
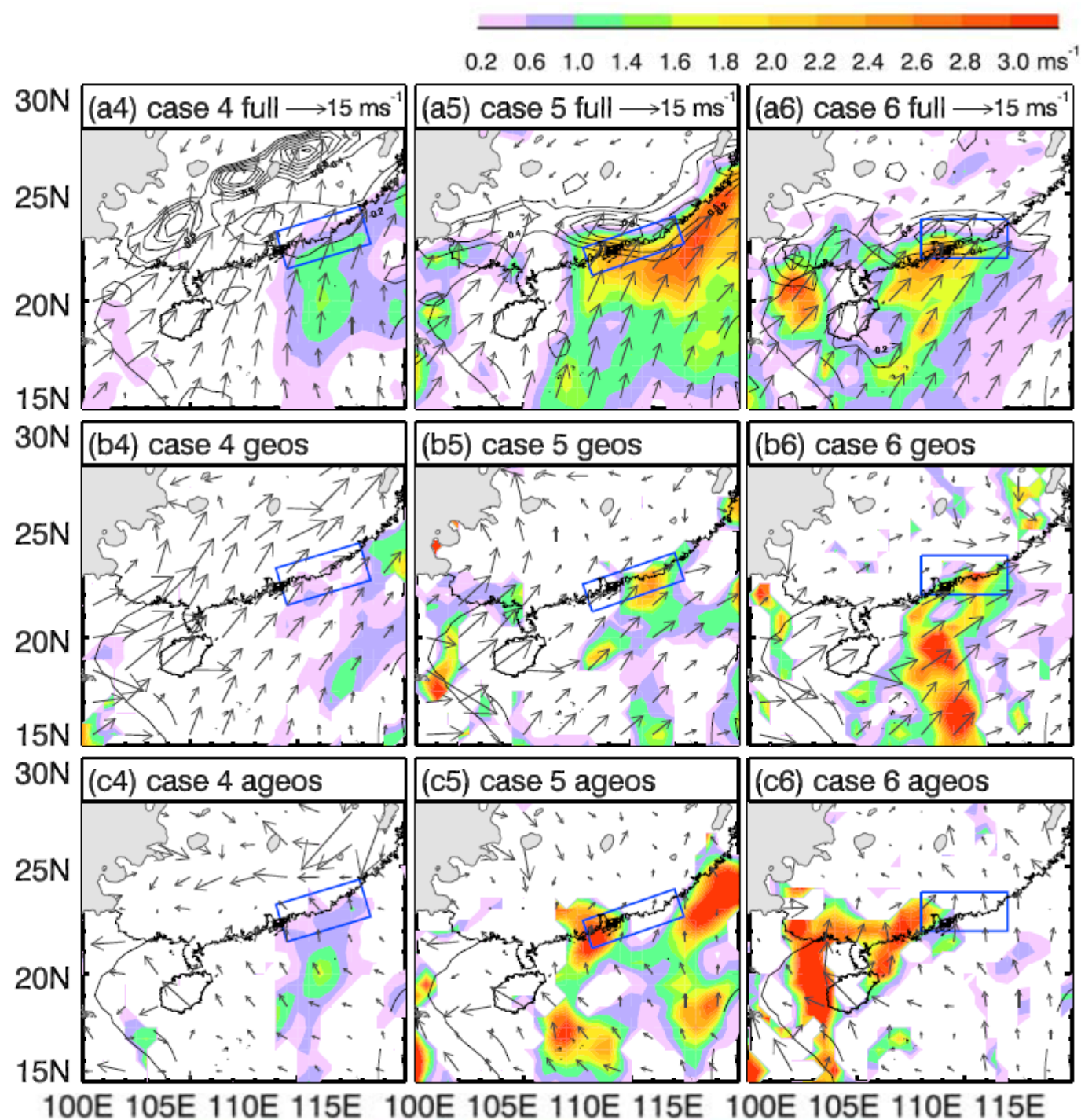
PC

Correlation between the PC and geopotential height at (a1–a6) 850 hPa and (b1–b6) 925 hPa at the starting moments of the model-data analysis periods of the six cases. Contours (at intervals of 10 gpm) represent the geopotential height from the good (solid) and bad members (dashed) at (a1–a6) 850 hPa and (b1–b6) 925 hPa.
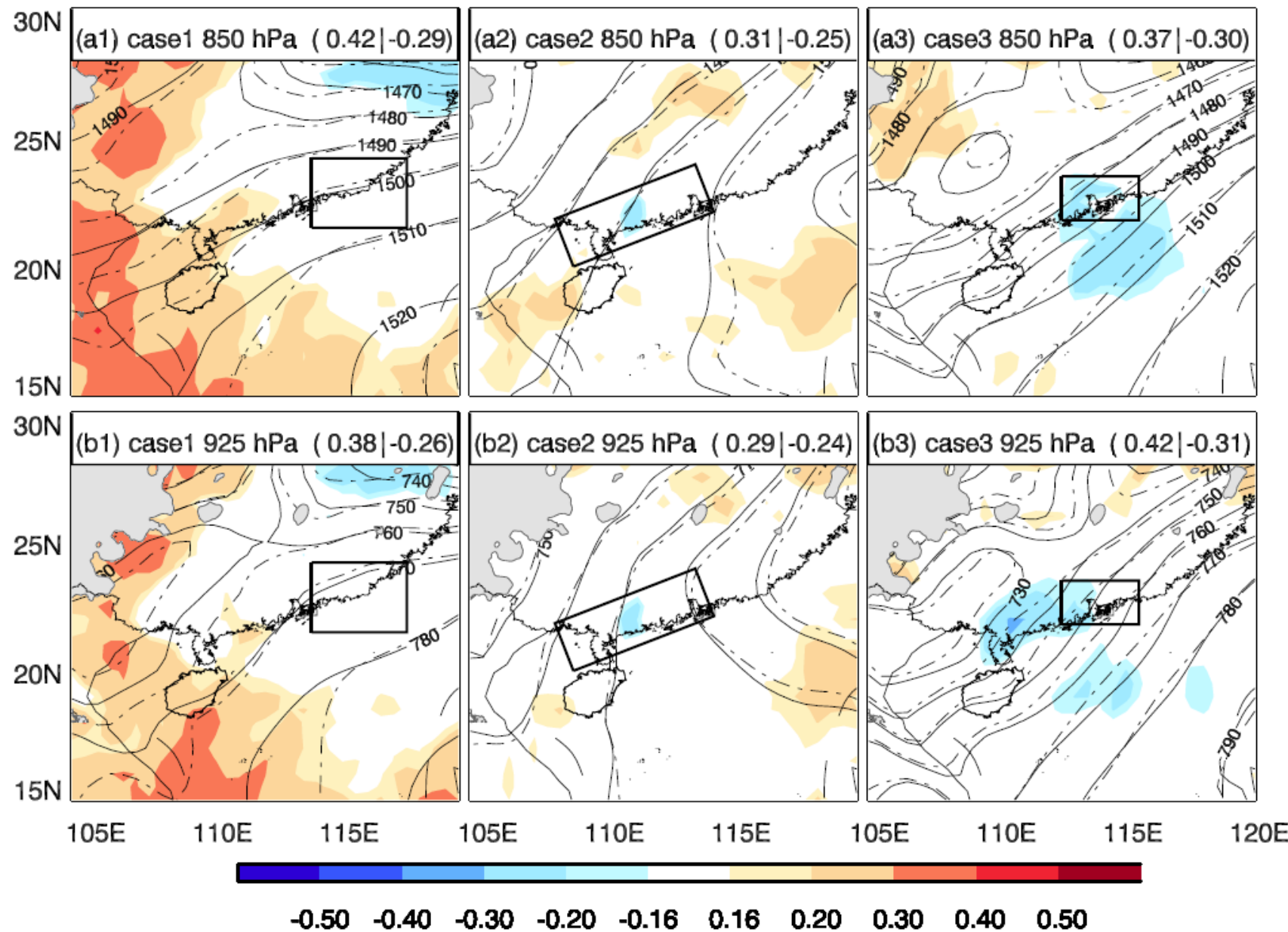
PC

- Case 3, 5, 6 the max. values of the positive geostrophic V differences near the coastal regions > 2.6 m/s

- Negative correlations between geopotential height and PC
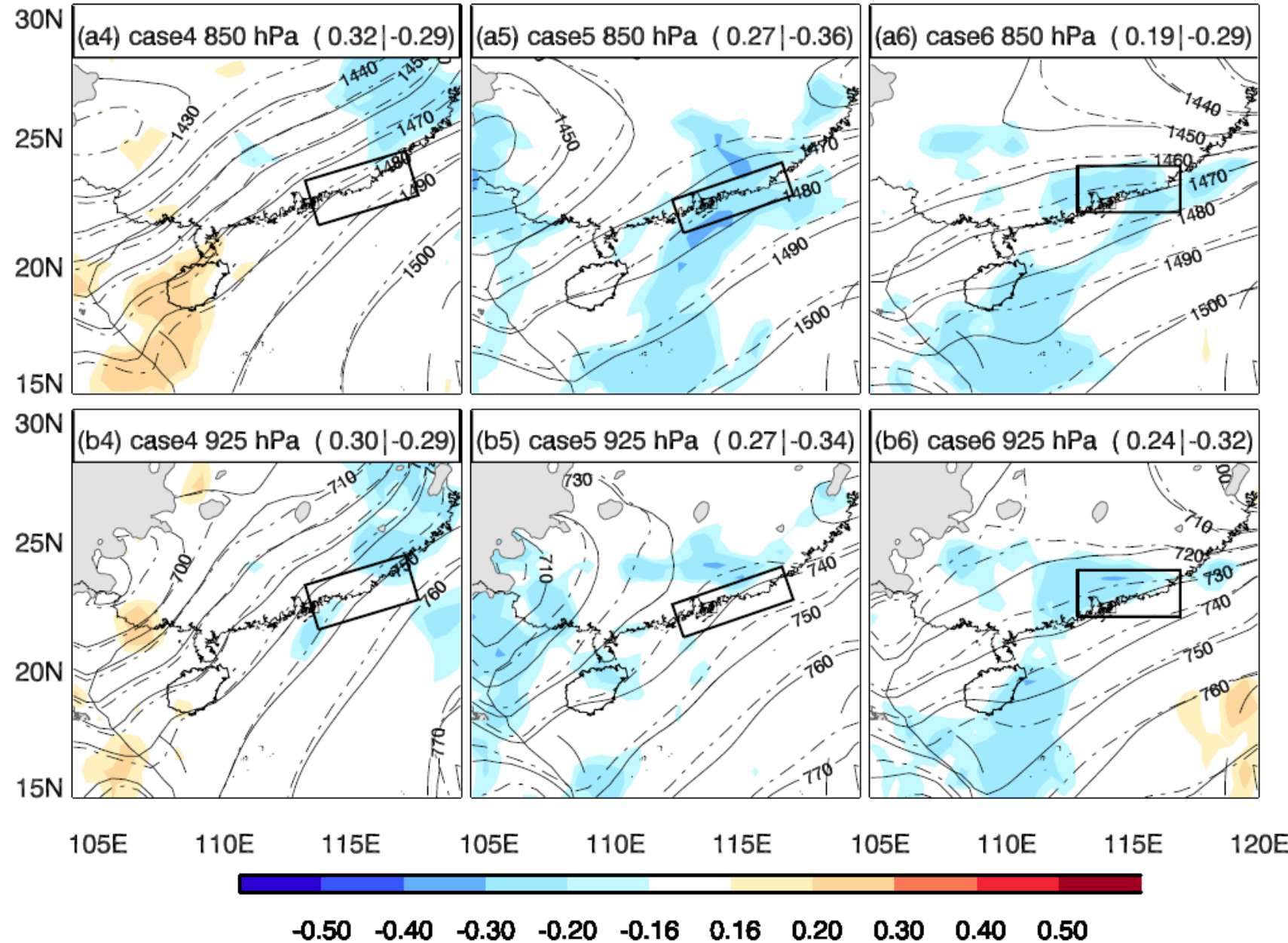
PC

- Deep column of strong quasi-geostrophic ascent in the good members

- Suggest that the subtropical low-pressure synoptic systems could be beneficial to the extreme PC.

- The ageostrophic meridional wind in the BLJs is an important dynamic factor for the coastal rainfall production, while the geostrophic meridional winds and associated front/shear line also play a nonnegligible but indispensable role.
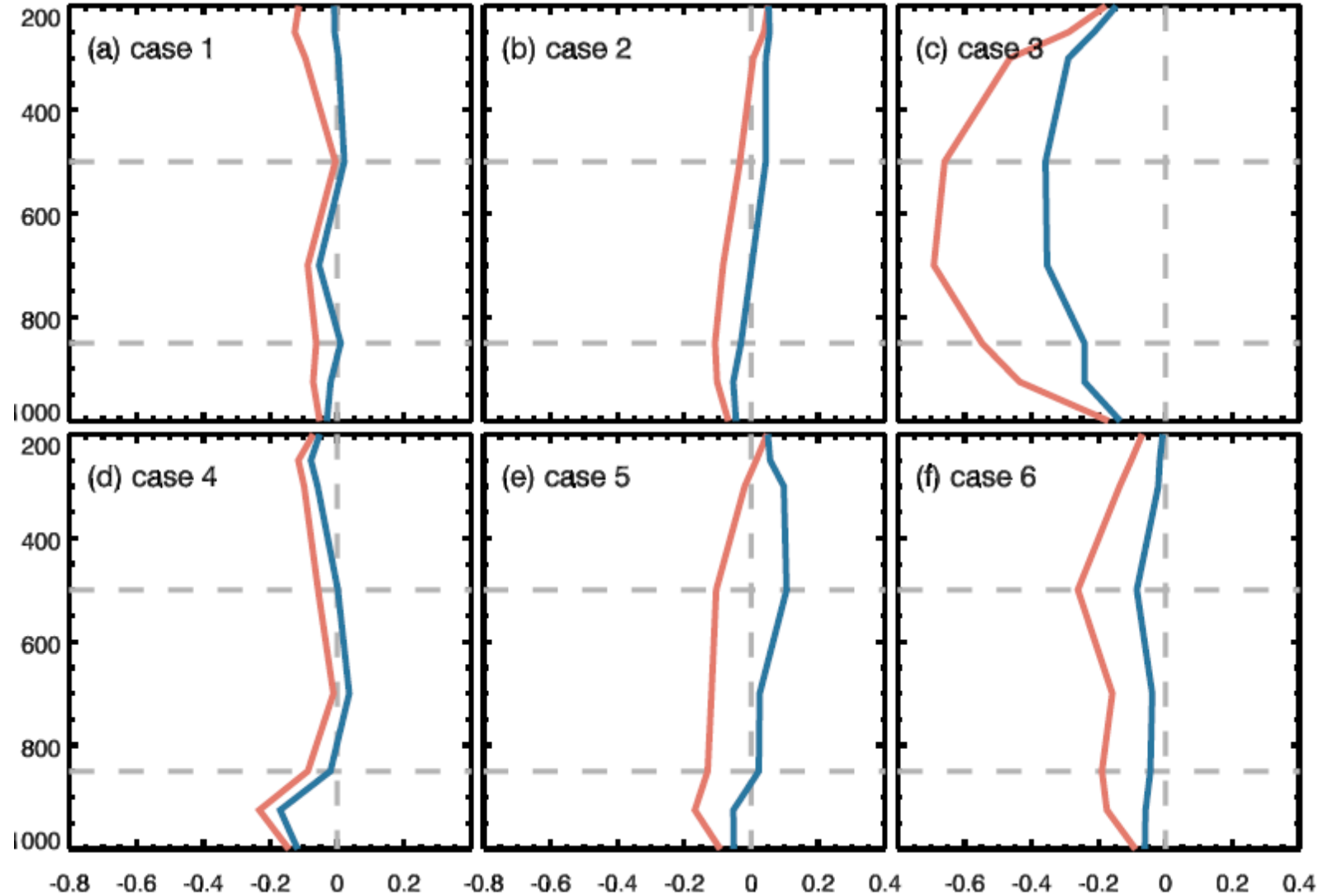
Figure 15. Vertical profile of area-averaged quasi-geostrophic vertical velocity (Pa s^{-1}) in the coastal regions for the (a–f) six cases, on the starting moments of the model-data analysis periods, from the good (orange) and bad (blue) members.

Conclusion

- The tropical-originating airflows in the BL and lower troposphere are important to the generation of the inland and coastal heavy rainfall over south China during pre-summer rainy season.

- Stronger SW SLLJs and BLJs contribute substantially to the PI production by enhancing convergence at their exit zones. The stronger southerly winds in the SLLJs are mainly contributed by geostrophic winds associated with stronger fronts, low-level vortices and shear lines.

- The major dynamic factor for the coastal heavy rainfall is mainly confined within the BL. Stronger southerly winds in the BLJs over the northern SCS lead to stronger convergence at their exit zones, which favors production of heavy rainfall over the coastal area of south China. Ageostrophic meridional wind in the BLJs is closely associated with the coastal rainfall production, indicating the importance of land-sea contrast and turbulent mixing in the BL.

- The lower predictability of coastal extreme rainfall might be attributed to the coarse resolution of the ECMWF global model.